INSTITUTO SUPERIOR TÉCNICO
Universidade Técnica de Lisboa

Functional Connectivity Measures in Memory Networks Using Independent Component Analysis

CATARINA SAIOTE FERREIRA LEITE

Master Thesis in

BIOMEDICAL ENGINEERING

Jury

Supervisor: Prof. Patrícia Margarida Piedade Figueiredo

President: Prof. Fernando Henrique Lopes da Silva

External: Prof. Alexandre Andrade

Prof. João Miguel Raposo Sanches

November 2009

Acknowledgements

I would like to thank to all the people without whom this work would not be possible.

Firstly, thank you to Prof. Patrícia Figueiredo, my supervisor, for all the suggestions in the development of this thesis, enthusiasm and support up to the last minute.

Also, to all the friends who kept me going on, I am thankful for their patience through the hardest times and for giving some of their time to help me revising. In particular, I would like to thank Joana L., Joana S., Lina, Marta and Sara for their precious friendship and help.

Finally, I am very grateful to my family for investing in my education throughout my life. A heartfelt “thank you” goes to my parents and brother, for the constant and unconditional support and motivation.

Abstract

Memory function consists of complex processes that appear to be compromised in several neurological pathologies. Consequently, memory processes have been the subject of diverse studies within the field of neurosciences, for instance, using functional magnetic resonance imaging (fMRI). Numerous methods have been developed to analyse fMRI data, not only to detect and localize activating areas, but most interestingly in order to assess functional connectivity between distinct brain regions.

The objective of this work was to explore methods of functional connectivity analysis of fMRI data using independent component analysis (ICA). The methods were applied to data from a previous study of memory function in normal subjects and patients with medial temporal lobe epilepsy and right hippocampal sclerosis (Figueiredo 2009). Three different group ICA approaches were tested: tensorial probabilistic ICA (PICA), PICA with temporal concatenation and ICA with temporal concatenation. Different pre-processing options were compared and methods were implemented to assist in the selection of components of interest.

Overall, different group ICA approaches were tested for the analysis of functional connectivity of fMRI data from two memory tasks. Functional connectivity was found in networks of brain areas involved in the performed tasks, as well as in networks commonly identified in resting-state fMRI studies. Moreover, significant group differences were observed between normal controls and patients and between younger and older subjects, which were consistent with comparable observations in the literature. The three ICA approaches yielded comparable networks, although, in general, the tensorial PICA approach proved more sensitive in the detection of group differences.

Keywords: memory networks, fMRI, functional connectivity, independent component analysis

Resumo

Uma das faculdades que frequentemente se mostra alterada em diversas patologias do foro neurológico é a memória. A memória engloba vários mecanismos complexos que são objecto de estudos diversificados em neurociências. Os estudos de Ressonância Magnética funcional (RMf) dispõem de diferentes métodos para análise dos dados, sendo possível, por exemplo, avaliar a conectividade funcional entre regiões do cérebro distintas.

Neste trabalho, procurou-se explorar métodos para analisar a conectividade funcional de dados de RMf, nomeadamente decomposição em componentes independentes (ICA). Foram utilizados dados de um estudo anterior (Figueiredo et al. 2008) sobre memória episódica em doentes com epilepsia do lobo temporal e esclerose do hipocampo.

Para este efeito, três métodos de ICA para analisar dados de grupo foram comparados: *probabilistic-ICA* (PICA) com uma abordagem tensorial, PICA com uma abordagem de concatenação temporal dos dados, e ICA com concatenação temporal. Opções diferentes de pré-processamento foram comparadas e desenvolveram-se métodos para ordenar e seleccionar as componentes de interesse.

No geral, identificaram-se redes com diferenças significativas entre grupos, não só comparando o grupo de controlo com os doentes, como também comparando grupos com média de idades diferente. Os resultados obtidos com os vários métodos de ICA foram semelhantes, embora a abordagem tensorial tenha detectado diferenças entre grupos mais significativas.

Em suma, os resultados das três abordagens de ICA para dados de grupo foram comparados. Foram desenvolvidos métodos para seleccionar as componentes e identificar diferenças significativas entre grupos.

Palavras-chave: redes de memória, MRf, conectividade funcional, decomposição em componentes independentes.

Index

List of Abbreviations

AD – Alzheimer's Disease

BET – Brain Extraction Tool

BOLD – Blood Oxygenation Level Dependent

COPE – Contrasts of Parameter Estimates

DCM – Dynamic Causal Modelling

EEG – Electroencephalography

EPI – Echo-Planar Imaging

FEAT – fMRI Expert Analysis Tool

FILM – FMRIB's Improved Linear Model

FLAME – FMRIB's Local Analysis of Mixed Effects

FLIRT – FMRIB's Linear Image Registration Tool

fMRI – Functional Magnetic Resonance Imaging

FMRIB – Functional Magnetic Resonance Imaging of the Brain

FSL – FMRIB's Software Library

FWHM – Full Width Half Maximum

GE – Gradient-Echo

GIFT – Group ICA of fMRI Toolbox

GLM – General Linear Model

GRF – Gaussian Random Field

HRF – Haemodynamic Response Function

IC – Independent Component

ICA – Independent Component Analysis

LFP – Local Field Potential

MCI – Mild Cognitive Impairment

MEG - Magnetoencephalography

MELODIC – Multivariate Exploratory Linear Optimized Decomposition into Independent Components

MNI – Montreal Neurological Institute

MTL – Medial Temporal Lobe

MTLE – Medial Temporal Lobe Epilepsy

MR – Magnetic Resonance

MRI – Magnetic Resonance Imaging

PE – Parameter Estimate

PET – Positron Emission Tomography

PICA – Probabilistic Independent Component Analysis

PCA – Principal Component Analysis

ROI – Region of Interest

RSN – Resting State Network

SPGR – Spoiled Gradient Recalled Echo

SPM – Statistical Parametric Mapping

SVD – Singular Value Decomposition

TE – Time of Echo

TR – Time of Repetition

List of Figures

List of Tables

1. INTRODUCTION

In today's neurosciences studies, data from several modalities is available. Functional magnetic resonance imaging (fMRI) is a widespread and valuable tool and it can be analyzed in a number of ways in order to provide different types of information regarding brain function. This work focuses on the investigation of functional connectivity across the brain using independent component analysis (ICA) methods. In particular, the application of such methodology to data from an episodic memory study is explored. In this Chapter, the theoretical background for the work developed in this Thesis will be presented, namely the basic principles underlying fMRI techniques and the major methods employed in analysis of the data. Also, results of relevant studies of memory function in the context of the developed project will be summarized. Finally, the goals of this work will be explained.

1.1. fMRI – Basic principles

Functional Magnetic Resonance Imaging (fMRI) is a type of Magnetic Resonance Imaging (MRI) technique, which uses the sensitivity of the Magnetic Resonance (MR) signal to changes in the brain haemodynamics in response to neuronal activity. It is a versatile and non-invasive technique and one of its advantages is to allow the study of the entire brain simultaneously. In this section, The basic principles of magnetic resonance (MR) signal generation will firstly be presented, as well as the mechanisms that generate image contrast in MR images. Then special attention will be paid to the generation of the blood-oxygen-level-dependent (BOLD) signal and its relation to neural activity.

1.1.1. MR signal generation

The constituents of atomic nuclei possess angular momentum, usually called spin. Therefore, atomic nuclei have a net angular momentum determined by the number of protons and neutrons which they are made of. Since atomic nuclei have positive electric charge, they exhibit a non-zero nuclear magnetic moment whenever the nuclear spin is non-zero. Nuclei that have even atomic number and even charge number have no spin and consequently no MR signal. Hydrogen nuclei show one of the strongest nuclear moments and are usually elected for biological studies with MRI. In what regards brain imaging, the signal arises mainly from hydrogen nuclei in water, where density is high enough to allow measurements with high spatial resolution.

In an MR experience, the sample is placed in a strong magnetic field, usually referred to as B_0. In this situation, spins align along the direction of the magnetic field, defined as the *z* or longitudinal direction, exhibiting a movement of precession around this axis. The hydrogen nucleus has spin of ½ and according to the quantum mechanical rules there are two energy levels in a magnetic field. The two energy levels correspond to either parallel or anti-parallel alignment. Since more spins will align in a parallel rather than anti-parallel fashion, there will be a net magnetization. This, however, produces no detectable signal as the net magnetization at equilibrium does not change over time. The signal that is used to obtain both MRI and fMRI images is detected by a conducting coil placed around the sample

and results from the perturbation of the magnetic dipoles with radiofrequency electromagnetic waves. This perturbation consists of a magnetic field B_1 transverse to B_0, alternating precisely at the Larmor frequency. This frequency depends on the substance and on the strength of the static magnetic field as described by the Larmor equation:

$$\nu = \gamma B_0 \quad (1)$$

The Larmor frequency is represented by ν and γ represents the gyromagnetic ratio of the nucleus. B_0 is the strength of the magnetic field.

If excited at this precise frequency, the spins change to a higher energy state creating a magnetization component in the transverse plane. When the B_1 field is turned off and the excitation is over, the hydrogen nuclei return gradually to the low energy state, which results in a variation of the transverse component of the magnetization that can be measured with the conducting coils. The rate at which the hydrogen nuclei return to the low-level energy state depends on the properties of the surrounding tissue and the physiological state of the brain, allowing us to create images.

The spin relaxation back to the low-energy state can be described as the recovery of longitudinal magnetization known as T_1 relaxation, and the decay of transverse magnetization termed T_2 relaxation. This corresponds to two exponential processes with time constants T_1 and T_2 respectively. T_1 relaxation is related with the re-establishment of thermal equilibrium. By exchanging energy with the surroundings or lattice, the spins return to equilibrium, which gives this process the alternative name of spin-lattice relaxation. The surrounding molecules cause small fluctuating magnetic fields which can have a component of motion in the Larmor frequency of the nuclei in the static field. This way the spins are allowed to alter their energy state realigning their magnetic moment with the longitudinal direction. The reason why different tissues have different T_1 relaxation times can be explained with how high the component of molecular motion at the Larmor frequency is, a property which varies with the molecular composition of the tissue. It should also be noted that T_1 relaxation times also depend on the strength of the main static field. As can be seen by the Larmor equation, if strength of the B_0 field is increased the Larmor frequency will also increase, resulting in longer T_1 relaxation times for both white and grey matter. The decay of transverse magnetization is known as T_2 relaxation or spin-spin relaxation because it involves only the phases of other nuclear spins. It is a consequence of local random field fluctuations at the molecular level causing some nuclei to vary the resonance frequency, gradually leading to a loss of the spin phase coherence until no net magnetization can be detected in the transverse plane. T_2 relaxation times are much less dependent on the static field strength since they are more sensitive to very slow molecular motions and not only to motions at the Larmor frequency. (Jezzard and Clare 2001)

The transverse relaxation would be correctly described by an exponential decay with time constant T_2 in an ideal homogeneous magnetic field. In physiological tissue that is not the case, since the tissue itself can respond differently to a perfectly homogeneous applied magnetic field. Particularly, regions with boundaries between tissues with different magnetic susceptibilities, like the air/tissue interfaces near the sinuses in the head, cause severe magnetic field variations. Because of the variations in the magnetic field the spins will not precess at precisely the same the same frequency, speeding the loss

of coherence and transverse relaxation. In this situation, the decay constant is termed T_2*, and is more significant to fMRI. In the brain, these field inhomogeneities depend on the physiological state of the brain, particularly on the composition of the local blood supply, which are related to the neural activity. That is why measurement of T_2* consists in an indirect measurement of neural activity. How these measurements are related will be addressed further on. (Jezzard and Clare 2001; Logothetis and Wandell 2004)

1.1.2. The BOLD Signal

The most commonly used type of contrast in fMRI is called blood-oxygen-level-dependent (BOLD) signal. As the name implies, the BOLD signal reflects changes in blood oxygenation. In blood, haemoglobin can be found attached to oxygen (oxyhaemoglobin) or without it (deoxyhaemoglobin). The former is diamagnetic while the latter is paramagnetic. Therefore, deoxygenated blood has greater magnetic susceptibility, meaning that the decay of transverse magnetization depending on T_2* will be greater compared to that of oxygenated blood. In the late 1980s, it was observed that deoxygenated blood caused a reduction of the MR signal in the adjacent space (Ogawa and Lee 1990). In short, MR sequences sensitive to T_2* decay can detect changes on blood oxygenation which can reflect neuronal activation (Huettel et al. 2004; Matthews 2001).

Following this discovery, a series of experiments were performed to help understand the BOLD contrast mechanisms. In an experiment in anesthetized rats it was verified that the metabolic demand for oxygen is necessary to obtain BOLD contrast (Ogawa et al. 1990). Also, the influence of changes in blood flow was investigated and it was observed that an increase in blood flow causes deoxygenated haemoglobin to be flushed away, being replaced by excessive oxygenated haemoglobin thus decreasing the BOLD contrast. It was therefore concluded that the BOLD signal depends on the balance between the consumption and supply of oxygen. It was, then, expected that increased neuronal activity would lead to a decrease in MR signal. However, it was the inverse effect that was observed. This is due to an increase in blood flow that over-compensates the increased consumption of oxygen. This mismatch led to further investigations to determine the coupling between neuronal activity and the blood oxygenation level. Some explanations have been suggested but until today a consensual model that explains the full mechanism is lacking (Huettel et al. 2004).

To compare changes in neuronal activity and the BOLD signal, it is useful to define the haemodynamic response function (HRF): the BOLD response to a stimulus of short duration, the temporal impulse response function. Although the shape of the HRF can vary across the cortex, according to the stimulus nature or between subjects, a typical HRF can be described. The first changes in the BOLD signal begin only 1 or 2 seconds after the stimulus, reaching a peak value 6-9 seconds after stimulus onset returning to baseline afterward. Prolonging the duration of the stimulus will cause the BOLD response to extend the peak into a plateau. Sometimes the BOLD signal decreases below the baseline, effect called post-stimulus undershoot (see Figure 1(a) below). Some studies (Menon et al. 1995) have reported a small decrease of the BOLD signal before starting to increase, called the initial dip (see Figure 1(b) below).

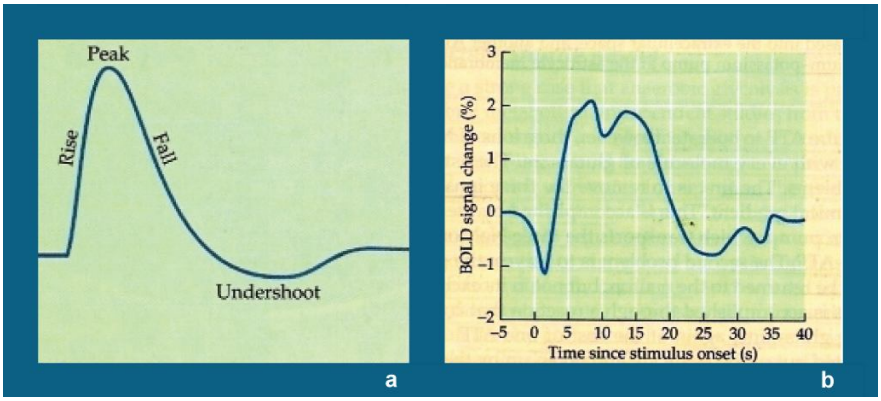

Figure 1. The HRF: (a) schematic representation of the BOLD response for a short-duration stimulus and (b) the BOLD response across all voxels with an initial dip. Adapted from (Huettel et al. 2004).

Studies with simultaneous fMRI and electrophysiological recordings have tried to establish a comparison between the electrical activity in the brain and observed BOLD signal. It has been stated that the BOLD contrast mechanism reflects primarily the neuronal input to the relevant area instead of the long range signals transmitted by action potentials to other regions. Also, comparisons of the amplitude of BOLD response at two locations may not correspond to the amplitudes of the neural signal in the same locations.

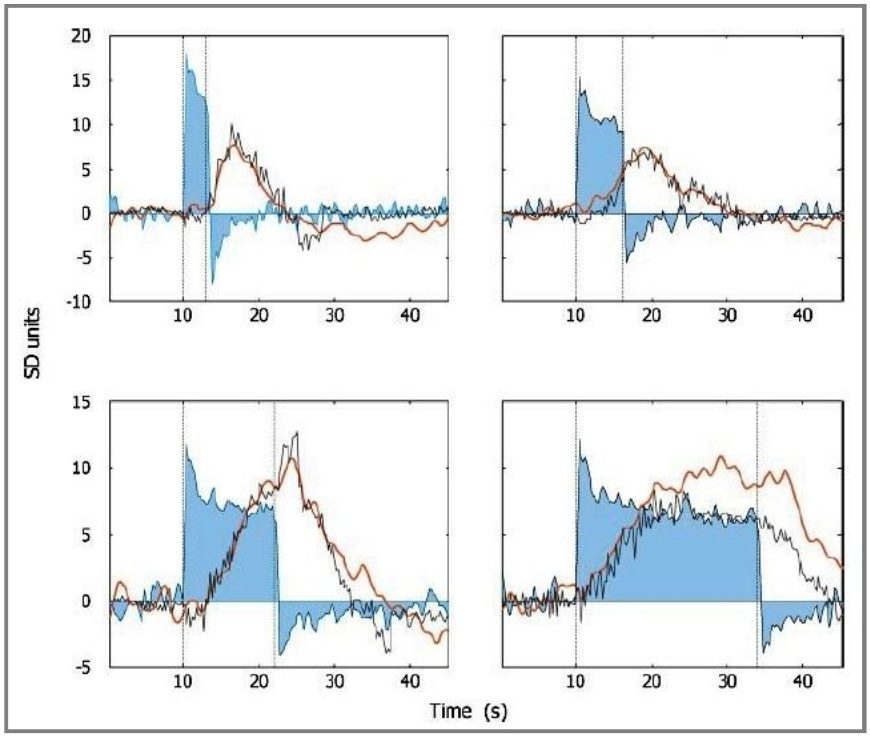

Figure 2. Simultaneous fMRI and intracortical recordings for visual stimuli of different duration: responses to stimuli of 3, 6, 12, and 24 s. Blue shaded trace: local field potentials (LFP); red trace: BOLD response; gray trace: predicted BOLD response after convolution of the LFP with the temporal impulse response function. Linear time invariant predictions are in good agreement over the duration range from 3 to 12 s, but not to the latter portion of the 24 s. (Logothetis and Wandell 2004)

It was also assessed that in the majority of situations the amplitude of the BOLD response is a linear but not time-invariant function of local field potentials (LFPs), multi-unit activity and firing rate of small populations. As stimulus durations increase it seems however that the relationship is not linear for the entire range of the response (see Figure 2 above). These studies concluded also that the LFP signal is a good correlate of BOLD response, which in fact increases when neuronal activity is augmented, with the drawback of limited linear relationship (Logothetis and Wandell 2004).

In spite of the limitations and of the indirect relation between brain activity and the measured signal, the BOLD contrast has become a widely used fMRI technique.

1.2. fMRI - Statistical Analysis

Typical fMRI data consists of scans acquired every few seconds, either during stimulation or at rest. Statistical analysis makes it possible to detect the parts of the brain where activity is increased (or decreased) due to the experimental stimulation. In order to maximize sensitivity and validity of the analysis, the fMRI data usually undergoes several pre-processing steps such as: reconstruction from k-space, slice-timing correction, motion correction, spatial smoothing, intensity normalization and low- and/or high-pass filtering of time series.

Several methods have been developed to analyze fMRI data. Methods that look at each voxel's time series independently are the most common and are said to be univariate methods. These include simple correlation analysis or the popular standard general linear model (GLM). Multivariate methods, on the other hand, try to make use of the spatial relationships that exist within the data. Analysis can also be divided into model-free (data-driven) and model-based methods. The former are exploratory and search for effects or components of interest in the data, whereas the latter compare the data with the model of the expected response to the stimulation. One popular data-driven method uses Independent Component Analysis (ICA) to find networks of functionally connected brain areas, which may or may not be correlated with the stimulus or task under study. This technique goes beyond the detection and localization of stimulus- or task-related activity, allowing the study of functional connectivity. Each type of method has advantages and disadvantages and the preference of one or another usually depends on the kind of study being performed. In the remaining of this section, a brief description of the GLM will firstly be presented. Afterwards, the various functional connectivity analysis and methods will be summarized and, finally, the basic principles of ICA methods will be described.

1.2.1. General Linear Model (GLM)

The general linear model describes the observed data as a linear combination of model functions, plus a noise term. For fMRI data this model is typically presented as follows:

$$\boldsymbol{X} = \boldsymbol{G}\,\boldsymbol{\beta} + \boldsymbol{e} \tag{2}$$

where $\boldsymbol{X}$ is the matrix containing the experimental data, with the time response of each voxel in its columns, $\boldsymbol{G}$ is called the design matrix in which the expected model functions are specified. Each row of the matrix constitutes a scan and each column contains a model effect. Model effects constitute expected changes in the BOLD signal. These can be effects of interest (related to the experimental hypothesis) or confounds (like scan artifacts) which are not related to the experimental hypothesis. The matrix $\boldsymbol{\beta}$ is the parameter matrix, which contains the parameter weights that indicate how much each model effect contributes to the observed data (see Figure 3 (a) below). The noise term is represented by $\boldsymbol{e}$. (Worsley and Friston 1995) In the course of the GLM analysis, the combination of parameters that minimizes the noise term is calculated, and the minimum error is called the residual. This are assumed to be independent and identically distributed as Gaussian noise. In the context of the GLM, the used cost function is the least-square errors, that is, the sum of the squared residuals across time. This value is used in the evaluation of statistical significance of a model effect: the amplitude of the corresponding parameter weight is divided by the residual error. Since this quantity follows an F-distribution under the null-hypothesis, it is possible to assess statistical significance according to the available degrees of freedom. (Huettel et al. 2004)

The GLM is the dominant tool for the analysis of fMRI data, useful in the evaluation of specific hypotheses in a given fMRI experiment. However, conclusions are drawn assuming a given model, and there is no guaranty that the model itself is appropriate. In addition, the method makes certain assumptions that may cause limitations in the conclusions withdrawn. For instance, the model assumes the design matrix is the same for all brain regions, but it is known that the HRF shows a different shape in different brain regions. This can be addressed by using multiple basis functions for the representation of the HRF or by performing an ROI analysis. Also, the GLM operates under the assumption that the noise level is independent of the task condition, that is, time invariant. However, it is usually observed that the noise level is higher during BOLD activity than at rest.

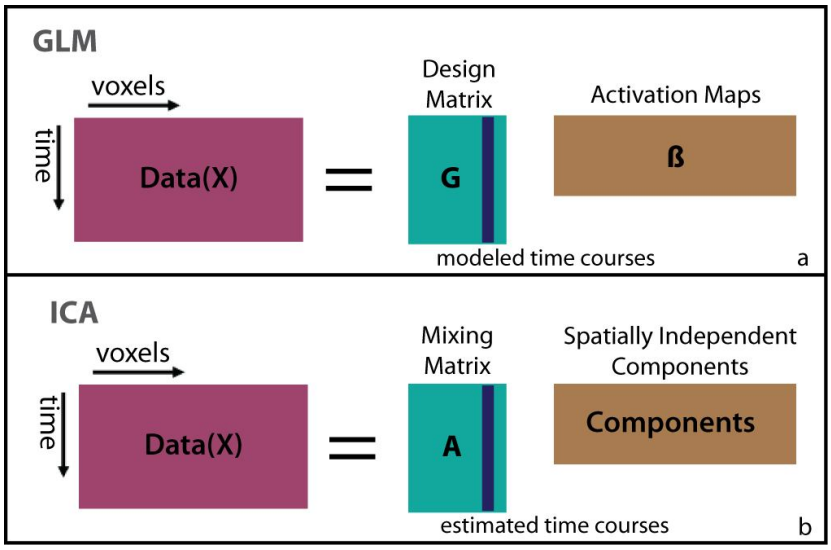

Figure 3. (a) In the GLM approach, a design matrix is constructed with the expected model effects and the estimated weight parameters yield spatial maps; (b) ICA estimates the time courses while searching for spatially independent components.

Finally, each voxel is analysed independently from all others, even though neighbour voxels usually share properties. Frequently, this is accounted for in later stages of the analysis by using diverse approaches for correction for multiple comparisons, such as Gaussian Random Field (GRF) theory or cluster-size thresholding (Huettel et al. 2004). Overall, the GLM approach is a powerful and flexible technique for testing a hypothesised model. However, situations exist in which there is no knowledge of an appropriate model and alternative approaches, such as data-driven methods like ICA (Figure 3 (b) above), have thus been developed.

1.2.2. Functional Connectivity Analysis

Early studies about brain function focused on identifying isolated brain regions that activated under a certain experimental condition. Nevertheless, it became progressively clear that this perspective was insufficient to account for the ability of the human brain to process information. For that reason, increasing attention has been paid to the conjoint activity of different brain regions: how they connect and interact with each other in order to perform a cognitive function. This is the subject of brain connectivity analysis (Li et al. 2008; Ramnani et al. 2002).

When connectivity is studied from the point of view of the temporal correlation between the activity of different brain regions, regardless of its anatomical basis, it is classified as functional connectivity. On the other hand, anatomical connectivity tries to determine the physical connections between brain regions. Effective connectivity is a type of functional connectivity measure that attempts to evaluate the influence that one brain region exerts on another: it is usually obtained by testing a pre-specified model based on knowledge of the underlying anatomical connectivity (Friston et al. 2003; Li et al. 2008; Ramnani et al. 2004).

The study of functional connectivity, as others studies with fMRI data, can be carried out with model-based or data-driven methods (see Figure 4 below). Model-based methods rely on prior knowledge or experience to select regions of interest (ROIs) and then search for other regions connected to these by using some metric of functional connectivity, such as cross-correlation, coherence analysis and statistical parametric mapping (SPM) (using GLM) (Li et al. 2008). Model-based methods often generate results easier to interpret. Regarding data-driven methods, these can be based on clustering analysis or decomposition techniques. Clustering analysis methods include fuzzy clustering analysis and hierarchical clustering analysis and their primary goal is to identify partitions of the data according to the proximity of the time-courses (Li et al. 2008). Methods based on decomposition techniques include principal component analysis (PCA), singular value decomposition (SVD) and independent component analysis (ICA). Both PCA and SVD methods attempt to decompose the data into a set of orthogonal components, each one made of a temporal pattern (called the principal component, since it corresponds to the direction of maximal variance) multiplied by the corresponding spatial map (the eigenimage). Frequently, PCA or SVD are used as a pre-processing step for dimensionality reduction before other analyses, such as ICA. Instead of searching for orthogonal components, ICA searches for statistical independence either in the spatial (spatial ICA) or temporal (temporal ICA) domains, which

seems to work better work for fMRI data (Calhoun et al. 2009; Li et al. 2008; Rogers et al. 2007). This method will be discussed in greater detail in the next section.

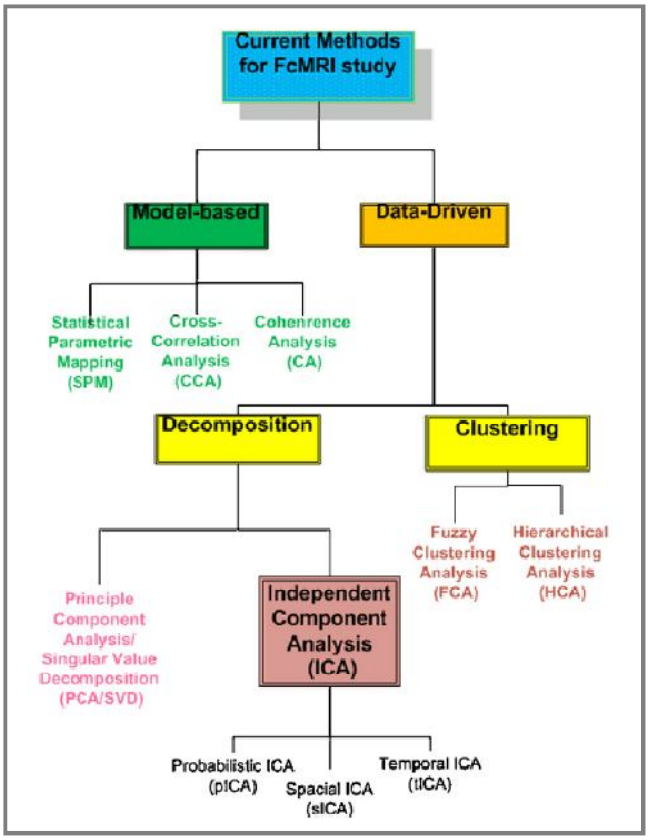

Figure 4. Methods used for the analysis of functional connectivity of fMRI data. Adapted from (Li et al. 2008)

Studies that perform functional connectivity analysis have been profuse in several fields of neurosciences research (Kincses et al. 2008; Ranganath et al. 2005; Summerfield et al. 2006) and, when combined with data from other approaches or modalities, may contribute significantly with important findings, particularly in clinical applications such as epilepsy or Alzheimer's disease (Bai et al. 2009; Rombouts et al. 2009; Voets et al. 2009; Wang et al. 2006).

1.2.3. Independent Component Analysis

Independent component analysis (ICA) is a data analysis and signal processing method used to estimate unknown source signals from a signal where they have been mixed together by an unknown mixing process, originally developed to solve problems that can be illustrated by the *cocktail-party problem*. This consists on trying to estimate two speech signals recorded by two microphones. Since the speeches were emitted simultaneously, the signals recorded by both microphones are weighted sums of the speech signals, and the weighting coefficients are unknown. It is however, possible to estimate such coefficients by using statistical properties of the original signals: it is enough to assume that the source signals are statistically independent. Currently, ICA has several applications, one of

them being to separate sources of brain activity either from electroencephalography (EEG), magnetoencephalography (MEG) or fMRI data (Hyvärinen and Oja 2000).

According to the general ICA model for fMRI data (McKeown et al. 1998), the observed data matrix $\boldsymbol{X}_{p\times n}$, where *p* is the number of time points and *n* the number of voxels, is generated by mixing *q* independent components:

$$\boldsymbol{X} = \boldsymbol{AS} \tag{3}$$

where $\boldsymbol{S}_{q\times n}$ is the matrix whose rows are statistically independent source signals or independent components (ICs). These are latent variables, since they cannot be observed directly, and assumed to be statistically independent and non-Gaussian. The mixing matrix $\boldsymbol{A}_{p\times q}$ is also unknown and it is precisely the goal of ICA to estimate it as well as $\boldsymbol{S}$. Usually $q \geq p$ and as a consequence $\boldsymbol{A}$ is of full rank. Each spatial map is associated to a time-course contained in the associate column of the mixing matrix. Once the mixing matrix is estimated, it is possible to obtain the independent components by computing its inverse:

$$\boldsymbol{S} = \boldsymbol{WX} \tag{4}$$

the unmixing matrix $\boldsymbol{W}$.

Since it was first applied to fMRI data (McKeown et al. 1998), ICA has been used in many applications and a number of algorithms have been developed. The most popular formulations are based on maximum likelihood estimation, maximization of information transfer, mutual information minimization and maximization of non-Gaussianity. The Infomax (Bell and Sejnowski 1995) and the Fixed-Point (Hyvärinen 1999) algorithms are amongst the most commonly used and both perform well, although the first tends to perform better in global model estimation and noise reduction while the latter is more accurate both spatially and temporally (Li et al. 2008). Several other algorithms have been developed (Calhoun et al. 2009).

ICA can be applied to fMRI data searching for independent components either in the spatial or temporal domains, but the latter approach has been far more common. Methods that attempt to combine both approaches have also been developed, for instance, by maximizing both spatial and temporal independence or by using spatial ICA to find regions of interest on which a temporal ICA is performed (Calhoun et al. 2009).

Generalization of ICA to the analysis of group data has also been the subject of great development. Unlike univariate methods, this generalization is far from obvious and therefore a multitude of approaches has been suggested that differ on the way group data is organized, the output available from the analysis and the method proposed to assess statistical significance. One of the ways to tackle group ICA consists on performing single-subject ICA and then make a posterior combination of the data into a group. Other approaches try to perform ICA directly on the group data. Among these, temporal concatenation yields common spatial maps and subject-specific time-courses while spatial concatenation results in the opposite situation. Subject-specific results in one domain can be viewed as an advantage since it allows straightforward comparison between subjects (Calhoun et al. 2001).

On the other hand, when searching for a common representation for the entire group, both in the temporal and spatial domain, the tensorial approach – Tensor Probabilistic ICA (*tensor-PICA*) (Beckmann and Smith 2005) seems more appropriate.

In its many approaches, ICA has been applied to the study of diverse aspects and may represent a source of complementary and relevant findings such as the study of memory function (Kincses et al. 2008; Ranganath et al. 2005; Summerfield et al. 2006), networks in epilepsy or Alzheimer's Disease (AD) (Bai et al. 2009; Rombouts et al. 2009; Voets et al. 2009), and resting state networks (RSNs) (De Luca et al. 2006; Wang et al. 2006).

1.3. Brain networks in memory function

Over the last decades, memory has become an object of intensive study in the field of neurosciences, not only because of the complexity of its mechanisms, but also due to the way it can be affected in several pathologies. The word memory may refer to several concepts and some common interpretations include: the capacity to encode, store or retrieve information, or the stored information itself. Memory encoding refers to the processing of sensory information and the ability to retain that information is called storage. Retrieval is the process of accessing stored information (Dudai 2002; Kandell et al. 2000). Each of these processes has different characteristics depending on the type of memory. Current classifications of memory systems typically distinguish between declarative or explicit memory (which can be consciously recollected and expressed in a statement) and non-declarative or implicit memory (related to motor or perceptual skills). Declarative memory can be further divided in semantic and episodic memory, and non-declarative memory includes several distinct processes (Squire 2004).

Several brain structures are known to play a role in episodic memory processes. The medial temporal lobe (MTL), for instance, includes structures such as the hippocampal formation, the parasubiculum and the entorhinal, perirhinal and parahippocampal cortices and evidence shows that it is essential for the establishment of long-term memory (Kandell et al. 2000). Since selective damage to each of these regions is rare in humans, lesion studies in primates have been used to determine the contribution of each structure. Also, tracer studies have been performed to determine the anatomical connectivity within the MTL region (Lavenex and Amaral 2000). Activation of the prefrontal cortex during memory tasks has been detected since the early nineties. Imaging studies with positron emission tomography (PET) and fMRI have frequently detected activations in this area highlighting its importance in memory processes. It has also been proposed that the role of prefrontal cortex in memory processes is related to the implementation of strategies in the memory tasks (Desgranges et al. 1998).

Being a complex cognitive process that involves multiple brain regions, memory function has naturally been the subject of multiple connectivity analyses. In some studies, it was found that functional connectivity (measured with correlation based methods) between chosen seed regions related to the task and other brain areas was a robust predictor of encoding success (Ranganath et al. 2005; Summerfield et al. 2006). In what regards clinical applications, cross-correlation analysis was also

used to assess connectivity between the hippocampus and other brain regions. Both a study involving patients with mild cognitive impairment (MCI) and another with patients suffering from Alzheimer's Disease (AD) observed decreased connectivity when comparing patients to controls (Bai et al. 2009; Wang et al. 2006). Recently, studies with ICA have also been performed. One study using tensor-PICA detected a decrease in functional connectivity of left medial temporal lobe epilepsy patients compared to controls, in a network containing the bilateral medial temporal lobes and other structures (Voets et al. 2009). Also, in a comparison between MCI patients and normal elderly controls, two out of six networks identified with *tensor-PICA* were more sensitive to differences between groups than model-based GLM analysis. Networks of activation and deactivation showed decreased activity in patients (Rombouts et al. 2009).

As shown, functional connectivity studies can contribute to gain additional knowledge on the subject of memory function. Additionally, exploratory methods allow the investigation of matters without prior model assumptions. For instance, the study of brain activity during rest is a typical example of studies where no model can be defined, as no particular stimuli are applied.

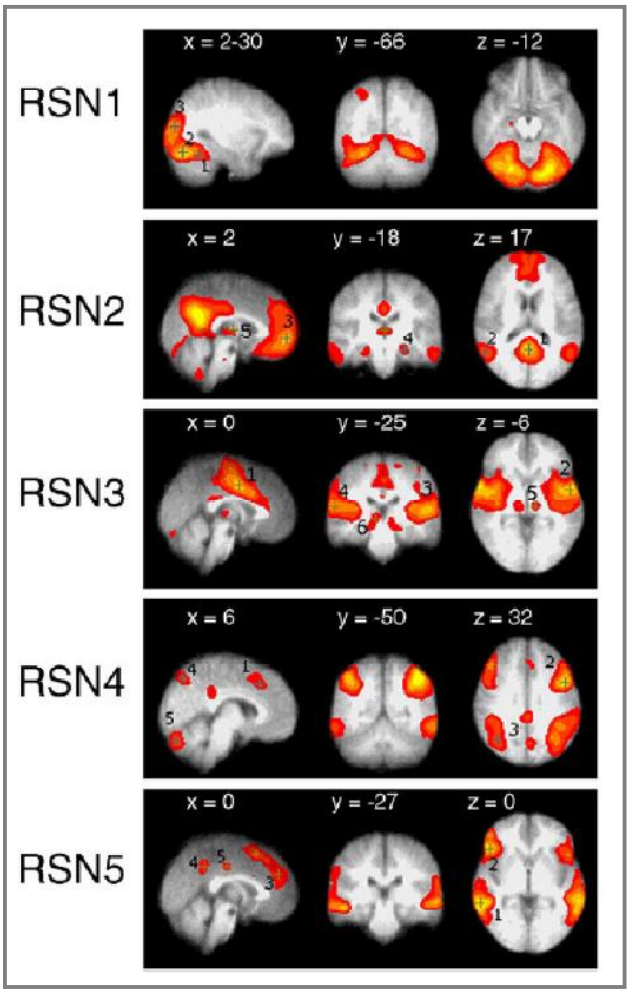

Figure 5. Group resting state network maps (map obtained with alternative hypothesis threshold P > 0.5). From top to bottom: (1) RSN 1 including the main visual functional network. (2) RSN 2 including visuospatial and executive system. (3) RSN 3 including sensory and auditory system. (4) RSN 4 including the dorsal pathway. (5) RSN 5 including ventral pathway (De Luca et al. 2006).

Even though the resting state condition lacks a precise definition, fMRI studies using the BOLD contrast have consistently observed fluctuations in the BOLD signal. These fluctuations have proved to be coherent across spatially separated brain regions that are functionally related, thus constituting resting state networks (RSNs) (see Figure 5 above) (De Luca et al. 2006). Several studies have used ICA to investigate the resting state since it does not require prior assumptions regarding a temporal or spatial pattern (De Luca et al. 2006). The RSNs include cognitively relevant functional networks and it has been seen that they can be altered in pathologies such as AD (Wang et al. 2006). Therefore, they can be a useful tool in the characterization of such states.

1.4. Aims of the current work

The main aim of this work was to explore methods for the analysis of functional connectivity. For this purpose, connectivity analyses were performed on data from memory encoding tasks, using ICA to search for components of interest and group differences.

Concerning the ICA methods, three approaches had to be compared:

- *tensor-PICA* (group ICA with a tensorial approach as implemented in MELODIC (Multivariate Exploratory Linear Optimized Decomposition into Independent Components));
- *concat-PICA* (group ICA with using temporal concatenation implemented in MELODIC);
- *concat-ICA* (group ICA with using temporal concatenation implemented in GIFT (Group ICA of fMRI Toolbox)).

The comparisons were meant to search for the approach that could better identify relevant source processes in the data, and eventually show more sensitivity in group comparison.

Furthermore, in the course of this work a method to sort relevant components from all the estimated sources was to be sought. Therefore, criteria were to be defined to select components of interest. Searching for group differences within the obtained networks was also a purpose of the present work.

2. MATERIALS & METHODS

In this thesis, methods for the analysis of functional connectivity in fMRI data using Independent Component Analysis (ICA) were explored. In particular, three different group ICA methods were tested and various component sorting methods were implemented, for the analysis of fMRI data previously collected from three groups of subjects in a study of memory function (Figueiredo et al. 2008). In this chapter, the data used will first be described and the functional connectivity analysis methods will then be presented.

2.1. fMRI data

Here, description of the subjects and their division into the considered groups will first be provided. Then, the paradigm of the memory task studied will be explained and the details about the data acquisition will be presented.

2.1.1. Subjects

Data were collected from a group of 20 healthy volunteers (CTRL), including 10 young (CTRL-Y) and 10 older adults (CTRL-O), and a group of 12 patients diagnosed with medial temporal lobe epilepsy (MTLE) with right hippocampal sclerosis (RTLE). All patients had active temporal lobe epilepsy with typical complex partial seizures and were on antiepileptic drug treatment. All subjects were right-handed and had normal or corrected to normal vision. Informed consent was obtained from each subject according to guidelines approved by our institutional ethical committee. Exclusion criteria for both patients and controls were: major depression, dementia, and other neuropsychiatric disorders. Subgroups were selected of 10 normal subjects (CTRL-M) and 10 patients (RTLE-M) matched for age and behavioural performance. This was assessed by recognition scores and average response times. Although education and gender may have an effect in memory function, the fact that the two groups have matched behavioural performance should control for such effects. For technical reasons, the data from the Verbal task of one of the older controls had to be excluded from the study.

Different sub-divisions of subjects into groups were considered in the various analyses approaches described below:

1. *All_subj* – all the subjects divided into controls (CTRL; n = 20) and patients (RTLE; n = 12) were included;
2. *All_subj_age* – subjects were subdivided into three groups: younger normal subjects (CTRL-Y; n = 10), older normal subjects (CTRL-O; n = 10) and patients (RTLE; n = 12);
3. *Matched_grps* – the subgroups of controls (CTRL-M; n = 10) and patients (RTLE-M; n = 10) matched for age and performance were considered;

4. *Matched_grps_perf* – the sub-group of patients was further divided according to performance: controls (CTRL-M; n = 10), patients with high performance (RTLE-H; n = 5) and patients with low performance (RTLE-L; n = 5).

2.1.2. Memory Paradigm

The subjects performed a Visual memory-encoding and a Verbal memory-encoding paradigm (Figueiredo et al. 2008). Each paradigm consisted of 10 cycles of one task block and one control block (see Figure 6). Each task block lasted 18 s during which 3 pairs of drawing/rotated drawing (Visual) or word/pseudowords (Verbal) were presented. Each block of 3 pairs was alternated with a control task of equal duration. In the visual task subjects were instructed to select the drawing aligned with the vertical or horizontal axis, whereas the verbal task consisted of identification of the real word. During the control task subjects were asked to identify the position of a black square (left or right). Each task consisted of 10 cycles of encoding task followed by control task. A recognition task followed approximately 10 min after encoding. Subjects were shown the 30 previously studied targets pseudo-randomly intermixed with 30 novel foils, for each material type, and were asked to make old/new judgments on each item through a button press.

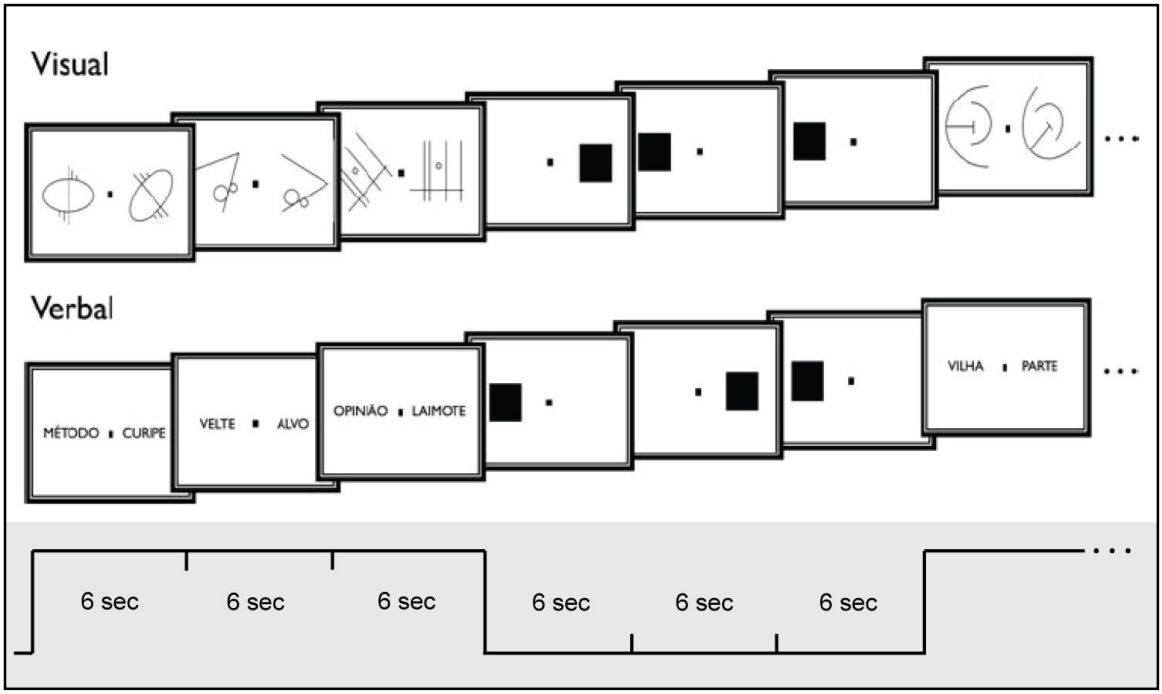

Figure 6. Schematic representation of the visual and verbal task paradigms. Each item is presented for 6 s. Blocks of 18 s are alternated with periods of control task of equal duration (black square in one of two positions). In total, 10 cycles of encoding and control task periods are presented. Adapted from (Figueiredo et al. 2008)

2.1.3. Image acquisition

The BOLD fMRI data were acquired on a 1.5 Tesla Philips Gyroscan Intera whole-body MRI system (Philips Medical System, Best, The Netherlands) using gradient-echo echo-planar-imaging (GE-EPI)

with the following acquisition parameters: repetition time (TR) = 3000 ms, echo-time (TE) = 50 ms, and flip angle 90º. A total of ~30 axial slices were obtained with ~4 mm thickness, ~240 x 240 mm^2 field of view, and 64 x 64 acquisition matrix, yielding a voxel size of ~3.5 x 3.5 x 4.0 mm^3. Each functional scan consisted of 120 volumes with a total duration of 360s (6min). To obtain T1-weighted structural images, a spoiled gradient recalled echo (SPGR) pulse sequence was used in the same session, with axial slices of 1 mm thickness, ~240 x 240 field of view and 256 x 256 acquisition matrix, yielding a reconstructed voxel of ~1 mm^3.

2.2. fMRI analysis

For the analysis of fMRI data, specially developed software tools were used, in particular: FSL (FMRIB's Software Library, www.fmrib.ox.ac.uk/fsl) (v4.12) and Statistical Parametric Mapping (SPM: www.fil.ion.ucl.ac.uk/spm). For ICA, the MELODIC (v3.09) and GIFT (v1.3g) tools were used, and Linux shell scripts were developed. In this section, the methods utilized to analyse the data will be specified, from the pre-processing steps, followed by the GLM and ICA analyses and posterior analyses.

2.2.1. Pre-processing

Pre-processing of fMRI datasets from both Visual and Verbal encoding tasks was carried out using FEAT (FMRI Expert Analysis Tool) Version 5.98, part of FSL and included:

- motion correction (see Figure 7 below) by co-registration of all volumes to a reference volume using MCFLIRT (Jenkinson et al. 2002);
- non-brain structures removal using BET (Brain Extraction Tool) (Smith 2002);
- spatial smoothing using a Gaussian kernel of 5.0 mm or 8.0 mm FWHM (Full Width Half Maximum);
- grand-mean intensity normalisation of the entire 4D dataset by a single multiplicative factor;
- high-pass temporal filtering (Gaussian-weighted least-squares straight line fitting, 50 s cutoff).

2.2.2. GLM Analysis

Data from each subject were entered in a (GLM) analysis with local autocorrelation correction using FMRIB's Improved Linear Model (FILM), to search for encoding-related activity changes (Woolrich et al. 2001). Regressors for each task consisted of a square function of width corresponding to the stimulus duration convolved with the canonical Gamma-variate haemodynamic response function (HRF). The first time derivative of the canonical HRF was also included in the model as a regressor, in order to account for any potential variability in the delay and dispersion of the haemodynamic response across the brain and between subjects. Also, six motion parameters (three of translational and three of rotational motion) were added as covariates of no interest, in order to account for any signal variability due to the detected motion (see Figure 8 below). The parameter estimates (PE) were

obtained by using a least squares algorithm. Linear contrasts of parameter estimates (COPE) between the visual and verbal encoding conditions and the control baseline were then calculated, yielding statistical maps of increased brain activity for each task and subject.

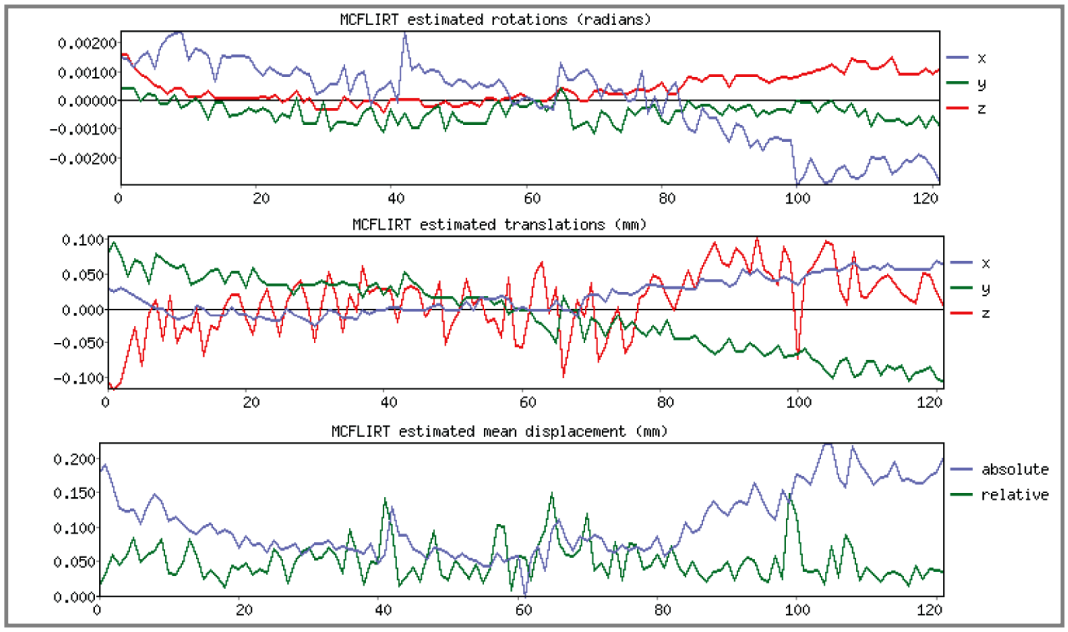

Figure 7. Example of the motion parameters (rotations, translations and mean displacement) estimated by application of a co-registration algorithm, for the motion correction step, in pre-processing of the data.

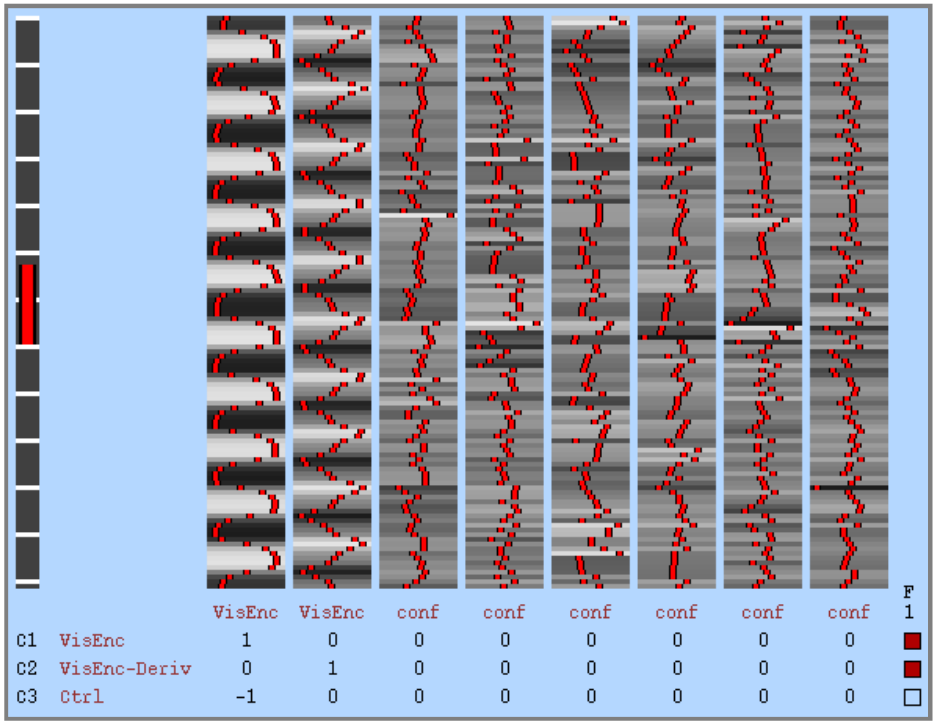

Figure 8. Example of the design matrix used for a first-level GLM analysis using FEAT. The first column corresponds to the task convolved with the HRF, the second to the first-derivative, and the last six correspond to motion parameters (covariates). Three COPEs were defined: *VisEnc*, *VisEnc-Deriv* and *Ctrl*.

Group analyses were carried out using FLAME (FMRIB's Local Analysis of Mixed Effects) - stage 1 (Beckmann et al. 2003; Woolrich et al. 2004), consisting on a mixed-effects (fixed and random effects) approach using Bayesian estimation techniques. Low-resolution functional images were registered to the corresponding high-resolution T1-weighted structural images of each subject. These were in turn registered to the Montreal Neurological Institute (MNI) template for a standard brain (Collins et al. 1994) with a resolution of 2 x 2 x 2 mm^3. Registration was carried out using FMRIB's Linear Image Registration Tool (FLIRT) (Jenkinson et al. 2002; Jenkinson and Smith 2001). For each task, the individual normalized COPE images were then entered into a second-level statistical analyses and the mean group effects were identified by one sample t-tests for each group. Contrasts were defined for group/subgroup comparisons.

Finally, Gaussian random fields (GRF) theory was used to accomplish maximum-height thresholding of the Z-score images at the significance level p = 0.05, corrected for multiple comparisons (Worsley 2001).

2.2.3. Independent Component Analysis

In this work, three different ICA implementations for group fMRI data were explored:

1. *tensor-PICA* (Tensorial Probabilistic Independent Component Analysis) in MELODIC/FSL;
2. *concat-PICA* (PICA with temporal concatenation) in MELODIC/FSL;
3. *concat-ICA* (ICA with temporal concatenation) in GIFT toolbox.

Even though, the first and second methods constitute two different approaches (tensorial and temporal concatenation) to group ICA, both are derived from the same method for single-subject ICA – probabilistic ICA (PICA). The GIFT implementation uses a different ICA algorithm and another method to assess statistical significance, but again uses a temporal concatenation approach for the analysis of group data. This section, thus, will begin by a brief description of PICA. Afterwards, the group ICA methods derived from PICA will be explained, along with the description of the analyses carried out in each case. Finally, the GIFT implementation will be summarized and performed analyses will be depicted.

2.2.3.1. Background – single-subject PICA

The original ICA model for fMRI data (McKeown et al. 1998) does not include a noise model, hence assuming that the estimated sources and the mixing matrix completely account for the observed data. This rules out the possibility of testing the estimated components for statistical significance within the framework of null-hypothesis testing. Also, the absence of a noise model makes any differences in the measured signal to be treated as valid spatial variations of the haemodynamic response, even it they arise solely from differences in the background noise. However, if the assumption on square mixing matrix is lifted, it is possible to consider a smaller number of source processes leading to a mismatch between the best linear model fit and the original data (Beckmann and Smith 2004). In the probabilistic

ICA (PICA) model, the mixing matrix is allowed to be non-square and the data are assumed to be confounded by additive Gaussian noise. It can be defined as follows:

$$\boldsymbol{x}_i = \boldsymbol{A}\boldsymbol{s}_i + \boldsymbol{\mu} + \boldsymbol{\eta}_i \quad (5)$$

where $\boldsymbol{x}_i$ stands for the *p*-dimensional column vector of individual measurements at i^{th} voxel, $\boldsymbol{s}_i$ is the *q*-dimensional column vector of non-Gaussian source signals and $\boldsymbol{\eta}_i$ represents Gaussian noise, $\boldsymbol{\eta}_i \sim N(0, \sigma^2\boldsymbol{\Sigma}_i)$. It is assumed that $q < p$, that is, there are fewer source processes than observations in time. The vector $\boldsymbol{\mu}$ denotes the mean of the observations $\boldsymbol{x}_i$ where the index *i* is over the set of all voxel locations *V* and the matrix $\boldsymbol{A}_{p\times q}$ is assumed to be of rank *q*. The goal is to find matrix $\boldsymbol{W}$ such that

$$\hat{\boldsymbol{s}} = \boldsymbol{W}\boldsymbol{x} \quad (6)$$

is a good approximation to the true source signals $\boldsymbol{s}$ (Beckmann and Smith 2004).

The process of estimating $\hat{\boldsymbol{s}}$ consists of three stages:

1) estimation of the number of components;
2) estimation of the independent components and noise;
3) evaluation of the statistical significance of the estimated sources.

In the first step, probabilistic PCA (Tipping and Bishop 1999) is used to find a linear subspace containing the sources and a noise subspace orthogonal to the first. It can be proved that only when analysis is performed in the appropriate *q*-dimensional subspace are the source processes uniquely identifiable (Beckmann and Smith 2004).

It is assumed that the noise model is isotropic and consequently the original time-courses need to be normalized to zero mean and unit variance as a pre-processing step. This places the data under the null-hypotheses of purely Gaussian noises. Therefore, in this stage only Gaussian noise is eliminated and any forms of structured noise (physiological noise, for instance) will probably show up as one of the estimated components. Nevertheless, as long as an activation and a physiological noise source processes are spatially distinct and not perfectly temporally correlated, they can be separated in the ICA process (Beckmann and Smith 2004).

The estimation of the number of sources is a problem of model order selection. This can be inferred from the covariance matrix of the observations using a Bayesian framework to approximate the posterior distribution of model order. Although the evaluation of the model order in the context of probabilistic PCA is usually based on the assumption of Gaussian source distribution, there is evidence that even when this is not the case, the Laplace approximation and the Bayesian Information Criterion yield consistent results (Minka 2000).

The second stage of the ICA process consists on estimating the components within the determined subspace. In the context of PICA, this is carried out using a fixed-point iteration algorithm that maximizes the non-Gaussianity of the source estimates using approximations to neg-entropy (Hyvärinen 1999).

The third step is used to assess the statistical significance of the estimated spatial maps. It has been argued that simply a transformation of the spatial maps into voxel-wise Z-scores (zero mean and unit variance) with subsequent thresholding results in an arbitrary false-positive rate. Instead, the individual IC maps can be converted into Z-statistic maps by performing a division of the raw IC maps by the estimate of the voxel-wise noise standard deviation. After that, Gaussian mixture modelling of the probability density of the spatial map of Z-scores is used in order to find out which voxels are significantly activated, with an alternative-hypothesis testing approach (Beckmann and Smith 2004).

All in all, PICA adds a noise model to the classical ICA applied to fMRI thus solving the problem of overfitting. The model is thus comparable to the standard GLM in that it assumes additive Gaussian distributed noise, differing in the number and shape of the regressors, which is estimated instead of specified a priori. This model is implemented as the MELODIC tool as part of FSL.

In the case of a GLM approach, multi-level analyses follow a hierarchical scheme: each level's results are combined into the next level's analyses estimates. Although this could be implemented for ICA techniques, exploratory approaches benefit from simultaneous analysis of all the data, which improves the ability to extract spatio-temporal modes of interest (Beckmann and Smith 2005). Thus, several models have been proposed for analysing group fMRI data in the ICA context, such as spatial or temporal concatenation and tensorial approaches (see Figure 9).

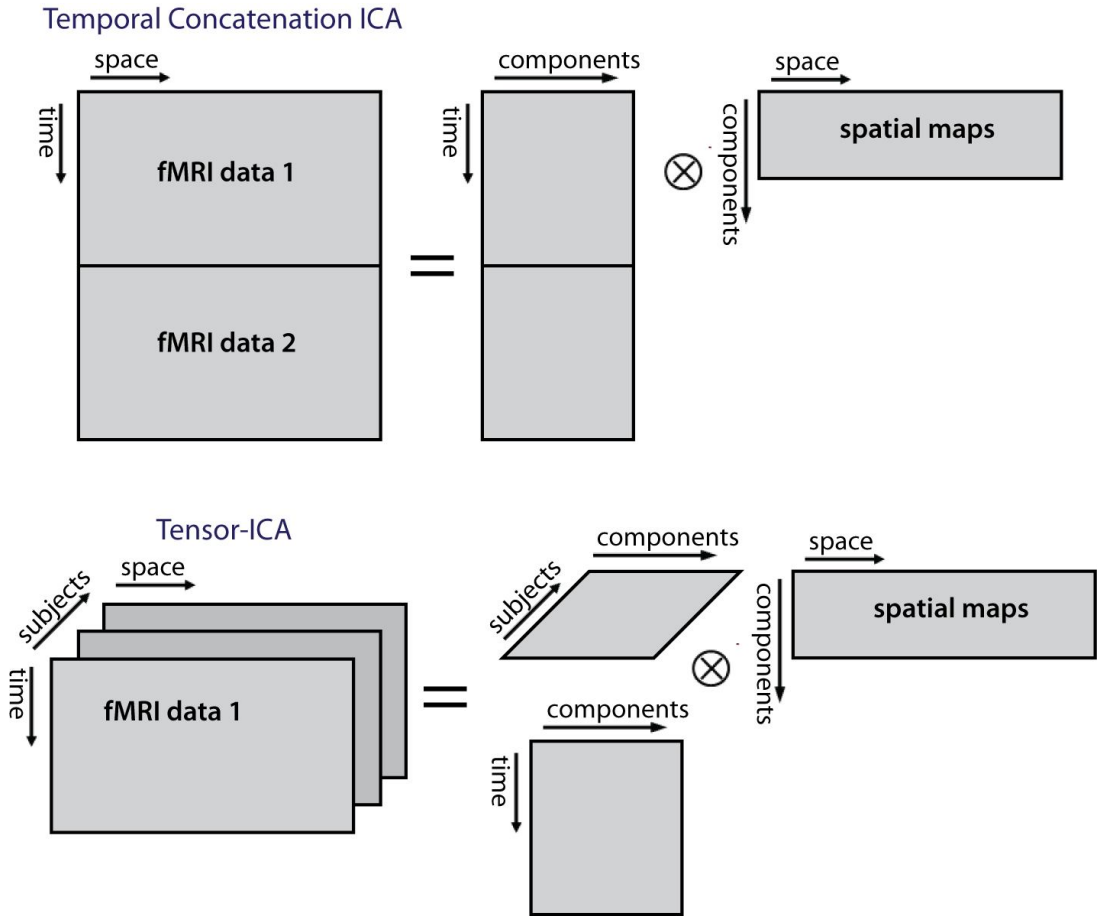

Figure 9. Schematic representation of two group ICA approaches: temporal concatenation and tensorial ICA.

Analysing fMRI data with an approach of spatial or temporal concatenation prior to the ICA decomposition yields time-courses that are common across subjects and subject-specific spatial maps or vice-versa in such a way that the multi-dimensional structure of the data is not reflected in the analysis. They allow, however, a simple comparison of subject differences within a component. The tensorial approach, on the other hand, allows the estimation of single spatial maps associated with single time-courses that together describe a source process across all subjects, bringing group ICA closer to group GLM analysis. *Tensor-PICA* yields a subject specific parameter as part of the IC decomposition, allowing subject comparison in this way.

Overall, the tensorial approach is preferable to the temporal concatenation approach when the stimulus paradigm is consistent across subjects, since it will try to estimate a single time-course across subjects for each component. However, it is not appropriate for the analysis of data where the subjects' time-courses are expected to be different, such as studies with a randomized design between sessions or resting state studies (Beckmann and Smith 2005; Calhoun et al. 2009).

2.2.3.2. Tensor-PICA

Tensorial Independent Component Analysis (*Tensor-PICA*) is a technique that extends single-session PICA to higher dimensions as an approach to multi-subject or multisession fMRI data analysis with ICA. This method is derived from Parallel Factor Analysis and results in a decomposition of the data into temporal, spatial and subject-dependent domains. Like in PICA, optimization for maximum non-Gaussianity of the estimated spatial modes is performed. The analysis steps are similar to the ones performed in PICA, with the addition of a pre-processing step meant to allow comparison of voxel locations between subjects: individual data-sets must be registered to a common space. Also the estimated spatial maps are thresholded as described for PICA (Beckmann and Smith 2005).

Analyses with *tensor-PICA* were performed corresponding to each one of the GLM group analysis as implemented in MELODIC Version 3.09, part of FSL (FMRIB's Software Library, www.fmrib.ox.ac.uk/fsl). Besides the pre-processing steps mentioned in 2.4.1, the following were applied to the input data:

- masking of non-brain voxels;
- voxel-wise de-meaning of the data;
- normalisation of the voxel-wise variance.

Pre-processed data were whitened and projected into the estimated subspace using probabilistic PCA, where the number of dimensions was estimated using the Laplace approximation to the Bayesian evidence of the model order (Beckmann and Smith 2004; Minka 2000). The whitened observations were decomposed into sets of vectors which describe signal variation across the temporal domain (time-courses), the session/subject domain and across the spatial domain (maps) by optimising for non-Gaussian spatial source distributions using a fixed-point iteration technique (Hyvärinen 1999). Estimated component maps were divided by the standard deviation of the residual noise and thresholded by fitting a mixture model to the histogram of intensity values (Beckmann and

Smith 2004). A GLM analysis was used to compare the estimates time-courses (one per component) with the task design. Additionally, since group analyses were performed, the estimated relative amplitudes for each subject (*subject mode*) were used to search for significant changes between the groups defined for the described second-level model-based analyses. This was carried out for each component using a GLM approach.

2.2.3.3. Concat-PICA (MELODIC)

The PICA-based group approach with temporal concatenation also requires co-registration of individual datasets to a common space and voxel-wise variance normalization and de-meaning is equally performed as a pre-processing step, as well as masking of non-brain voxels. Analyses were run for *All_subj_age* and *Matched_grps* sets previously described. An initial data reduction step is performed by projecting each dataset onto a common PCA eigenbasis, calculated from the mean data covariance matrix. The resulting datasets are then temporally concatenated and follow the same steps delineated for PICA. As performed in the *tensor-PICA* analyses, the time-courses were compared with the task design, to find the components best related to the task. However, unlike the tensorial approach, *concat-PICA* estimates one time-course per subject for each component. Therefore, the GLM analysis is performed using the best rank-1 approximation to the time-courses. The estimated responses in the *subject mode* were used to test for group differences as described for *tensor-PICA*.

2.2.3.4. Concat-ICA (GIFT)

The same pre-processed data were entered into analysis with the GIFT Matlab toolbox, using only the spatially smoothed data with a Gaussian kernel of FWHM = 5 mm. Although the GIFT implementation also follows a temporal concatenation approach, it differs from the model described above in some aspects (Calhoun et al. 2001).

The toolbox allows for estimation of the number of sources using the Akaike's Information Criterion / Minimum Description Length criterion (Akaike 1974; Rissanen 1983) and this was applied to one subject, yielding less than 20 components. The number of components was therefore fixed to the same number of components as obtained with MELODIC, that is, 20 for the Visual task including all the subjects and 19 for the Verbal task. The concatenated data were reduced to this dimension using PCA and then entered into the independent component estimation stage. Here, the Infomax algorithm (Bell and Sejnowski 1995) was used, which attempts to minimize mutual information.

After that, the GIFT approach includes a back-reconstruction step that yields time-courses and spatial maps for each subject. This is achieved by multiplying the partition of the unmixing matrix that corresponds to each subject's data with the corresponding partition of the data. The mean and standard deviation of each component was then calculated across subjects as well as the corresponding *t*-maps (Calhoun et al. 2001). These were thresholded at a level of significance $p = 0.05$. The components' time-courses were compared to the GLM design using multiple correlation analysis.

2.2.3.5. Component sorting

As implemented in MELODIC, the median response amplitude across subjects was computed for each component and they were ordered in decreasing order of this value. As mentioned, in all *tensor-PICA* and *concat-PICA* analyses, the estimated time-courses were used in a regression analysis against the GLM design, to identify any components that might be related to the task. Regarding the *concat-ICA* analyses, the relation of the components with the task was evaluated by testing each component's time-course against the GLM design, using temporal multiple regression.

To sort the components of interest obtained with *tensor-PICA* for further analysis, a group of criteria were thought of that would ensure the components were task-related and relevant across all the subjects. Thus, components should:

(i) be significantly related to the GLM design ($p = 0.05$);
(ii) have positive response amplitude for all the subjects.
(iii) Additionally, components clearly corresponding to motion artifacts were excluded by visual inspection.

Once the components of interest were identified, they were used to perform another round of *tensor-PICA* analyses that might be more sensitive to group differences. A script (in Appendix I) was written to create a mask derived from each of the components of interest, apply it to the pre-processed data of the corresponding task (*Visual* or *Verbal*) and run MELODIC. Since the automatic dimensionality of the data could be compromised by the incomplete data, each analysis was also carried out with reduction to the fixed number of 20 and 10 components. The same post-processing steps were applied as described for the previous *tensor-PICA* analyses.

3. RESULTS

In this chapter, the results obtained for the performed analyses will be presented. To begin with, the results for the higher-level GLM analysis will be summarized. After that, results for the ICA will be presented: first the *tensor-PICA* results, then the *concat-PICA* results, followed by the *concat-ICA* results. Finally, the results of the methods applied to sort the components will be described.

3.1. GLM – Second-Level Analyses

Group analyses of the Verbal and Visual memory tasks revealed activation of networks of brain areas in accordance with the previous study using the same datasets (Figueiredo et al. 2008). The whole-brain activation maps obtained for the Control group are shown in Figure 10.

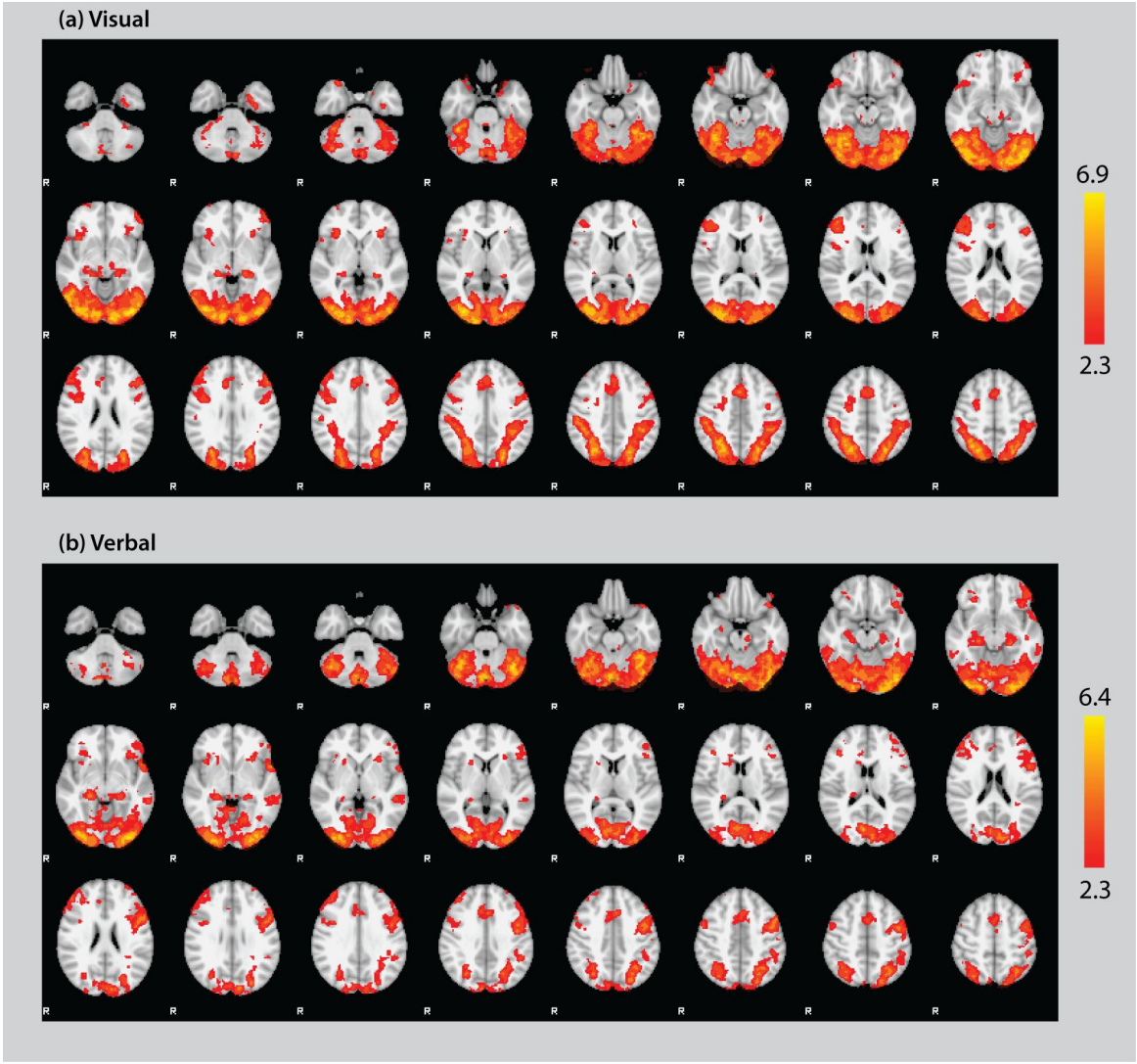

Figure 10. Activation maps obtained for the Control group for the group *All_subj* analysis using the GLM (FWHM = 5 mm) of: (a) Visual; and (b) Verbal tasks. Statistic images were thresholded using a (corrected) cluster significance threshold of p = 0.05.

Group analyses for all the subjects yielded no significant differences in activity between CTRL and RTLE or between CTRL-Y and CTRL-O groups. Similarly, the *Matched_grps* and the *Matched_grps_perf* analyses yielded no significant differences in activity between CTRL-M and RTLE-M or between the RTLE-H and RTLE-L groups. These results are in accordance with those reported in a previous study using the same datasets, where only an ROI analysis focusing on the MTL revealed contra-lateral shifts of activity in patients relative to controls (Figueiredo et al. 2008).

3.2. ICA Analyses

Regardless of the group approach utilised, all the ICA analysis yielded components showing activations in expected regions, considering the task, as well as components related to residual motion artifacts and other components harder to interpret. Results for each analysis will be described in greater detail in this section. All the data were registered and transformed to MNI standard space and all images show the components overlaid on the MNI template for a standard brain (T1 contrast structural image with non-brain structures removed) with a resolution of 2 x 2 x 2 mm^3. The coordinates in the spatial maps are given in mm.

3.2.1. *Tensor-PICA* results

Group analyses with *tensor*-PICA were performed using spatial smoothing with a Gaussian kernel of FWHM = 5 mm and FWHM = 8 mm. The number of independent components estimated for each *tensor-PICA* analysis is summarized in Table 1. Analyses carried out with spatial smoothing with a Gaussian kernel of FWHM = 5 mm yielded more components of interest than with FWHM = 8 mm. Therefore, in all subsequent results FWHM = 5 mm is used.

Table 1. Total number of independent components estimated for each tensor-PICA analysis.

	Visual Encoding		Verbal Encoding	
	FWHM = 5 mm	FWHM = 8 mm	FWHM = 5 mm	FWHM = 8 mm
All_subj	20	13	19	14
All_subj_age	20	13	19	14
Matched_grps	18	12	15	13
Matched_grps_perf	18	12	15	13

A summary of all the components identified in the *All_subj_age tensor-ICA* analysis for the Visual Encoding task is depicted in Figure 11 (a). Components were sorted in decreasing order of the median response per component (Figure 11 (b) below). Spatial maps were thresholded at $p > 0.5$ for an alternative hypothesis testing (voxels with more than 50% chance of not belonging to the background noise are above threshold).

Components 1 to 4 show task related networks, while component 5 is a typical example of a residual motion artifact.

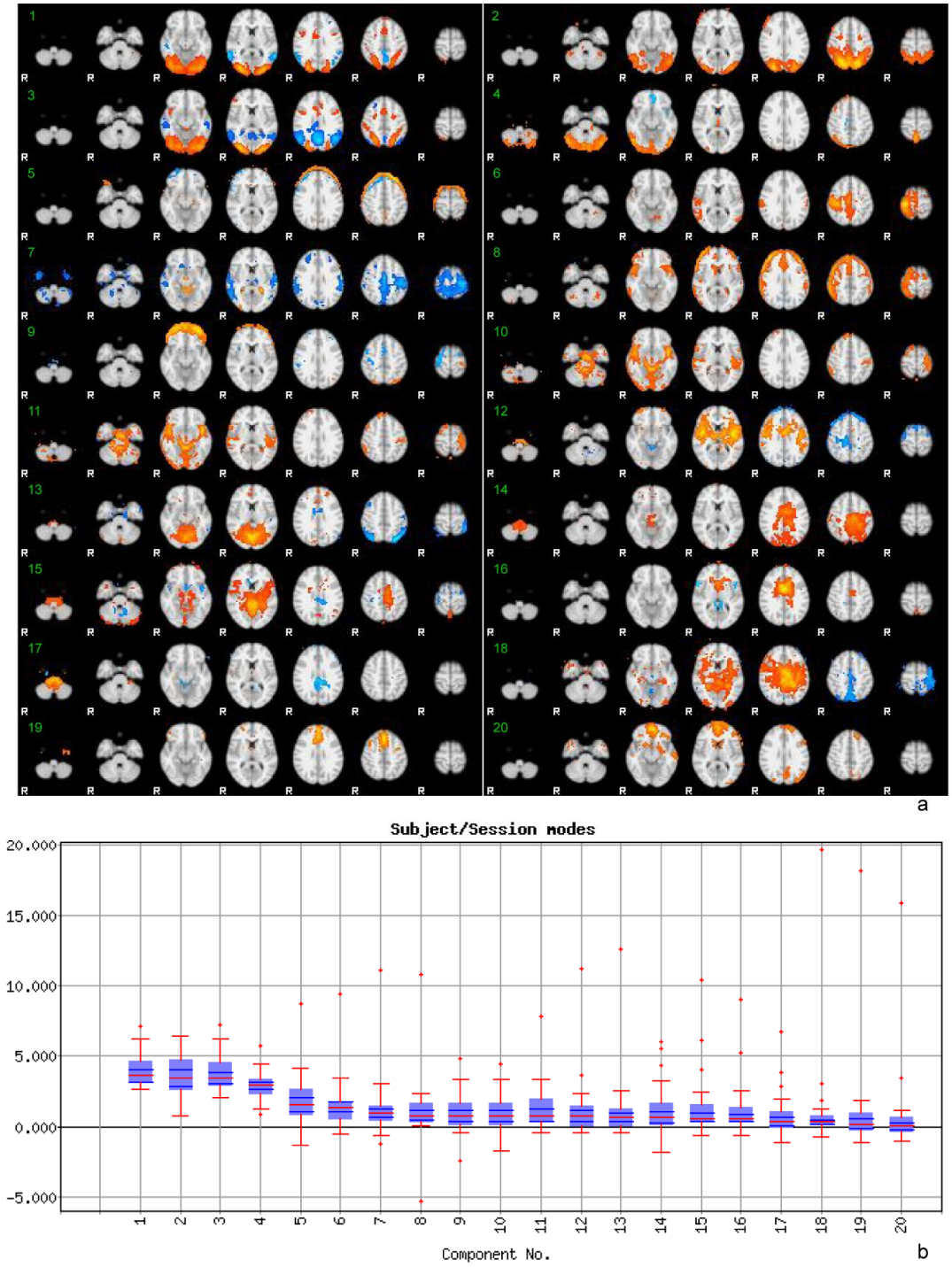

Figure 11. Output for *tensor-PICA* analysis *All_subj_age* for the Visual task (FWHM = 5 mm): (a) 20 components were identified (from left to right, axial slices for z = -52 mm, -32 mm, -12 mm, 8 mm, 28 mm, 48 mm and 68 mm): regions in red-yellow and regions in blue-lightblue are inversely correlated. Maps were threshold at P > 0.5 for (alternative hypothesis threshold for activation versus null); (b) amplitude responses in the subject mode per component ordered by decreasing value of median of responses.

ICA decomposition is blind to the phase of the time-courses of the components, therefore their sign is arbitrary and hence positive (red-yellow) and negative (blue-lightblue) components are inter-changeable. In fact, the positive component can be either correlated or inversely correlated with the

task, in which case the negative component would be inversely correlated or correlated with the task, respectively.

The subject-mode revealed, for all analyses of the Visual Encoding data, four components that showed (i) significant correlation with the task and (ii) positive relative amplitude in the subject mode for all the subjects. As for the Verbal Encoding, the *All_subj* analysis yielded two components matching both criteria while three components were obtained with each of the other analyses.

The components of interest obtained for each analysis are similar and therefore only those obtained for the *All_subj_age* analysis will be described in detail and shown (Figure 12 for the Visual task and Figure 13 for the Verbal task). The anatomical regions were identified by using the labeled MNI standard space structural image available in FSLView v3.1 Atlas tools (Collins et al. 1994; Mazziotta et al. 2001).

The components of interest obtained for the Visual task are shown in Figure 12. IC1 (14.45% of explained variance) shows activations in the visual areas, including both the dorsal and ventral pathways. The network also includes small regions of the primary auditory cortex (Heschl's gyrus), primary motor cortex (frontal pole) and parietal cortex (supramarginal gyrus and parietal operculum).

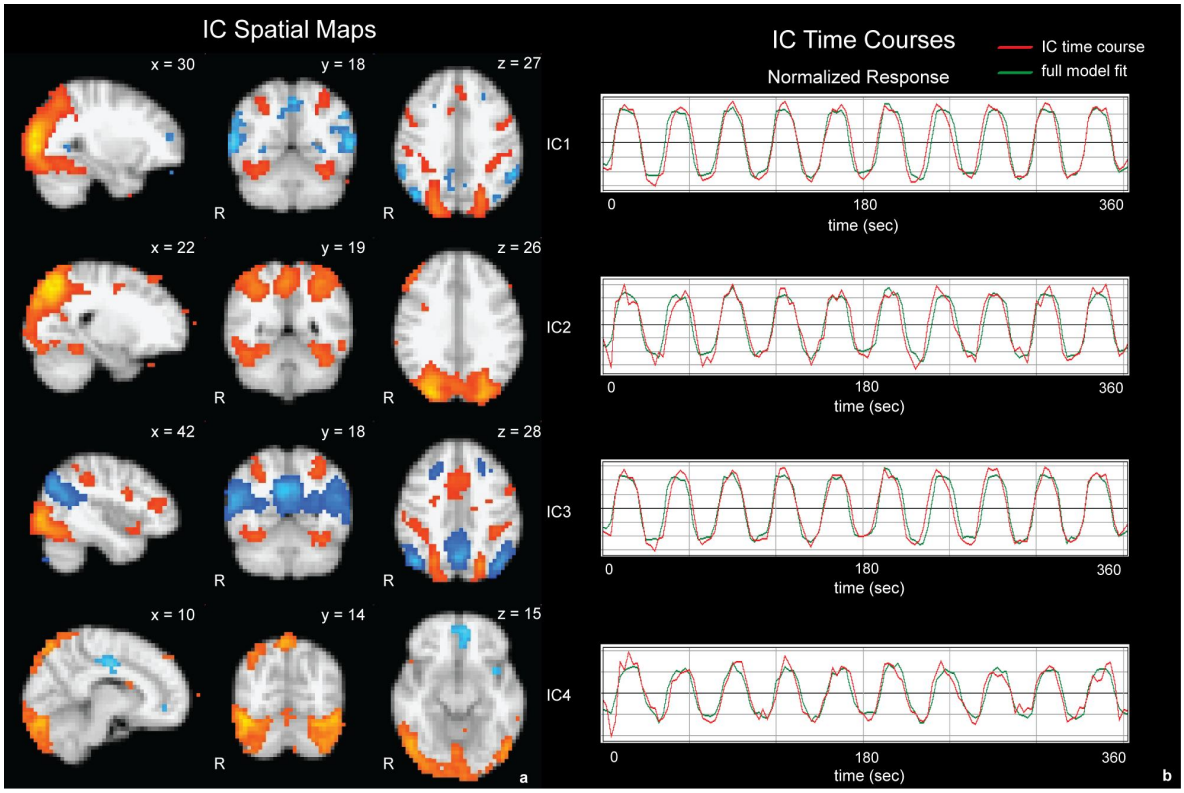

Figure 12. Components of interest (IC1, IC2, IC3, IC4) for *tensor-PICA* analysis (FWHM = 5 mm) of Visual Encoding task *All_subj_age*.(a) Spatial maps (alternative hypothesis threshold at p >0.5 for activation versus null) showing regions positively correlated with the task (red-yellow) and inversely correlated with the task (blue-lightblue); (b) time-courses of each component in red and the full model fit to the specified GLM design.

Additionally, IC1 contains regions whose time-course is inversely correlated with the task (in blue-lightblue in Figure 12) in the lateral occipital cortex and parietal cortex (supramarginal, angular and middle temporal gyri and precuneus) that correspond to a resting state network (RSN) described in the literature (De Luca et al. 2006). IC2 (13.85 % of explained variance) includes mainly posterior regions, including the visual areas, as in IC1, but more extensively activated in the parietal cortex. The third task-related independent component (13.80 % of explained variance) is very similar to IC1 regarding the regions with positive values, differing in the regions where deactivations were identified. These include the cuneus and precuneus, parietal regions (angular gyrus), lateral occipital cortex, the middle temporal gyrus and the frontal lobe, which form the RSN2. IC4 (11.63 % of explained variance) presents activations in inferior posterior regions of the occipital cortex mostly, also in the cerebellum, and deactivations in small frontal and parietal areas. The four described components' time-courses show significant correlation with the task (Memory>Control) at $p < 0.00001$.

Corresponding results for the Verbal task are presented in Figure 13. The component (14.60 % of explained variance) with highest median of responses in the subject mode is similar to IC1 described for the Visual task, with activations in visual areas slightly less extensive. In addition, it includes a lateralized region in the left frontal cortex including Broca's area, the frontal orbital cortex (OFC), middle frontal gyrus and precentral gyrus. IC2 (12.81 % of explained variance) comprises regions on the inferior and middle occipital and temporal cortices, frontal pole and also in the left and right hippocampus and parahippocampal gyrus. IC3 (12.40 % of explained variance) consists of regions in the primary visual area V1, intracalcarine cortex and lateral inferior occipital cortex, and also regions in the lingual gyrus and temporal occipital fusiform cortex.

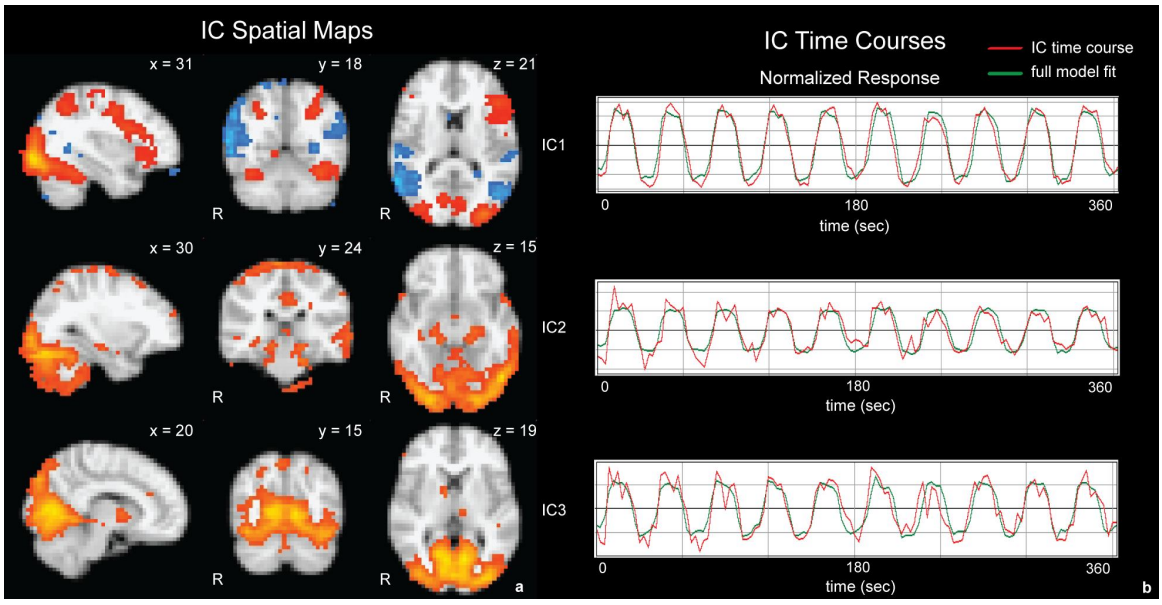

Figure 13. Components of interest (IC1, IC2, IC3) for *tensor-PICA* analysis (FWHM = 5 mm) of Verbal Encoding task *All_subj_age*. (a) Spatial maps (alternative hypothesis threshold at p >0.5 for activation versus null) showing regions positively correlated with the task (red-yellow) and inversely correlated with the task (blue-lightblue); (b) time-courses of each component in red and the full model fit to the specified GLM design.

The *All_subj* analysis yielded very similar components. In the Visual task, the four components of interest are the same but a shift in the order of second and third components occurred. The Verbal task analysis yielded two components of interest that correspond to the described IC1 and IC2 respectively. This was expected since the data is the same as in *All_subj_age*, the only difference being the post-statistics regarding group comparisons.

Regarding the analyses with groups matched for age and performance, the first component obtained for *Matched_grps* and *Matched_grps_perf* is similar to the described IC1, either in the Visual and Verbal tasks. The third component of *Matched_grps* and the fourth of *Matched_grps_perf* can both be compared to IC2 of *All_subj_age* for the Visual task, while the fourth and third components yielded by *Matched_grps* and *Matched_grps_perf* respectively, are similar to IC4. The second component in the matched groups' analyses output shares some features with IC2 from *All_subj_age*, but lacks the posterior deactivations that constitute RSN2, showing instead more extensive frontal deactivations. For the verbal task, the second component in both analyses is similar to IC2 described for the Visual task with less extensive activations. However it does not correspond to any of the identified components of interest for *All_subj_age* analysis of the Verbal task. The third component consists mainly of regions in the inferior occipital cortex, with no deactivations, in *Matched_grps* as well as *Matched_grps_perf*.

Significant changes between groups for each component were assessed using a GLM approach on each subject's relative response amplitude across the subject domain. None of the *tensor-PICA* yielded any component with significant changes ($p < 0.05$) between the defined groups either for the Visual or Verbal tasks. This is in accordance with the results of the standard GLM second-level analysis.

3.2.2. *Concat-PICA* results

The temporal concatenation approach was carried out in *All_subj_age* and *Matched_grps* analyses. In *All_subj_age* only one component of interest (see Figure 14 (a) below), similar to IC1, was obtained. More components significantly related to the GLM design were identified, but all showed at least one negative value in the amplitude responses in the subject mode. It is, however, worth mentioning the fourth component identified in *All_subj_age* analysis. It comprises solely regions that are inversely correlated with the task, similar to the deactivations in described IC3 from *tensor-PICA* analysis, corresponding to RSN2. Interestingly, this component shows significant differences (Figure 14 (b) and (c) below) between the CTRL-Y and CTRL-O groups ($p < 0.022$). The only two subjects with negative values in the subject mode of this component are considered outliers.

Concerning the Verbal Encoding task, only the first component matched the criteria for being considered a component of interest. It is similar to IC1 described for the tensorial approach.

The analysis *Matched_grps* yielded three components of interest for the Visual task and one for the Verbal task. In both situations, the first component is similar to IC1 in the corresponding analyses. The second component for the Visual task is similar to IC3 from *Matched_grps* analysis using *tensor-PICA*

and the third component is made up of the same regions as the fourth component of temporal concatenation *All_subj_age* analysis. None of the components show significant group differences either between normal subjects and patients or regarding age differences within normal subjects.

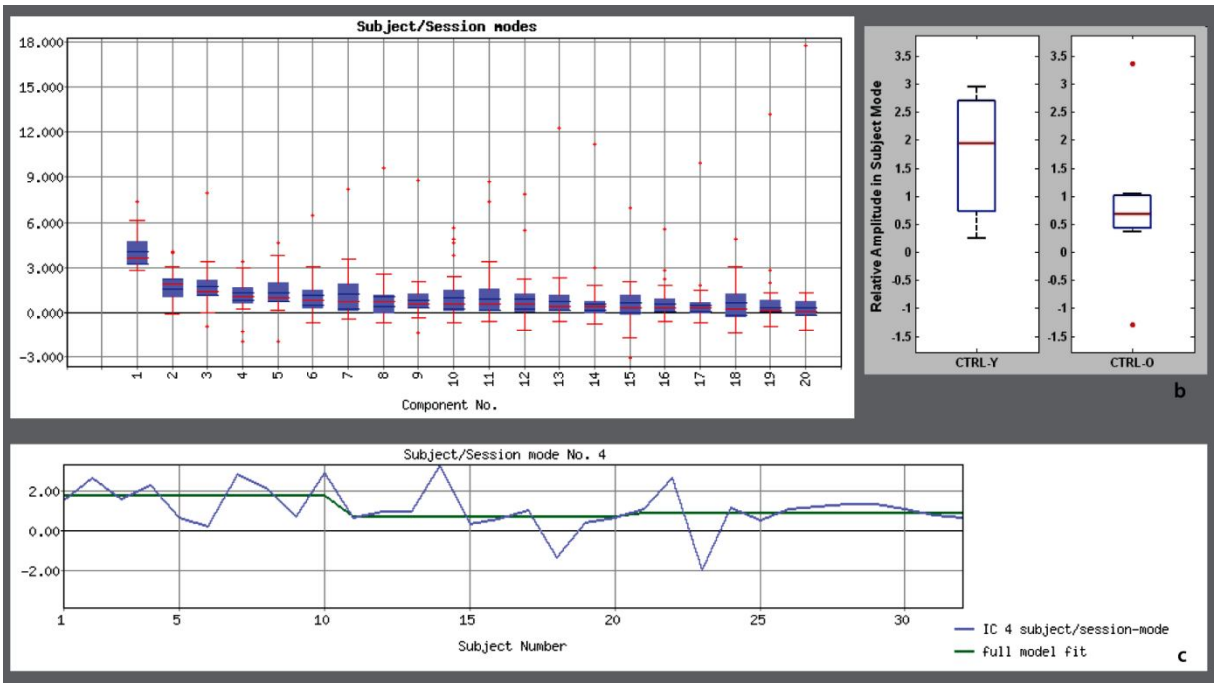

Figure 14. Subject modes for *All_subj_age* analysis of the Visual task using *concat-PICA* (FWHM = 5 mm): (a) Boxplots of the subject modes for the 20 components; (b) Boxplots for relative amplitude in subject mode in the first component, for subjects in CTRL-Y and CTRL-O groups; (c) comparison of the subject-specific value for the groups CTRL-Y (subjects 1-10), CTRL-O (subjects 11-20) and RTLE (subjects 21-32).

3.2.3. *Concat-ICA* results

Using the temporal concatenation approach as implemented in GIFT, yielded components comparable to those obtained with MELODIC. The components were ordered by decreasing order of correlation with the task assessed by multiple regression analysis between the GLM design and each component's time course. It can be seen in Figure 15 (below) that the component that showed strongest correlation with the GLM design (r = 0.4167) is similar to described IC1. The second component (r = 0.1697) does not correspond to any of the components of interest described for the previous analyses. Even though it was present among the identified components in some analyses, some of the amplitude responses in the subject mode were below zero. The following component (r = 0.1327) is similar to the third component obtained from *All_subj_age* analysis with temporal concatenation carried out in MELODIC whereas the fourth component (r = 0.1016) strongly resembles IC2. The last depicted component (r = 0.0769) is similar to the component with deactivations IC4, with additional frontal deactivations, thus comprising RSN2.

In what regards the verbal task (see Figure 16 below), the first component (r = 0.3121) corresponds to IC1. The second best task-related component (r = 0.0913) is composed of regions close to the ones

described in IC2. The third component (r = 0.0634) also corresponds to components yielded by the analyses run in MELODIC, although it did not match the criteria for component of interest.

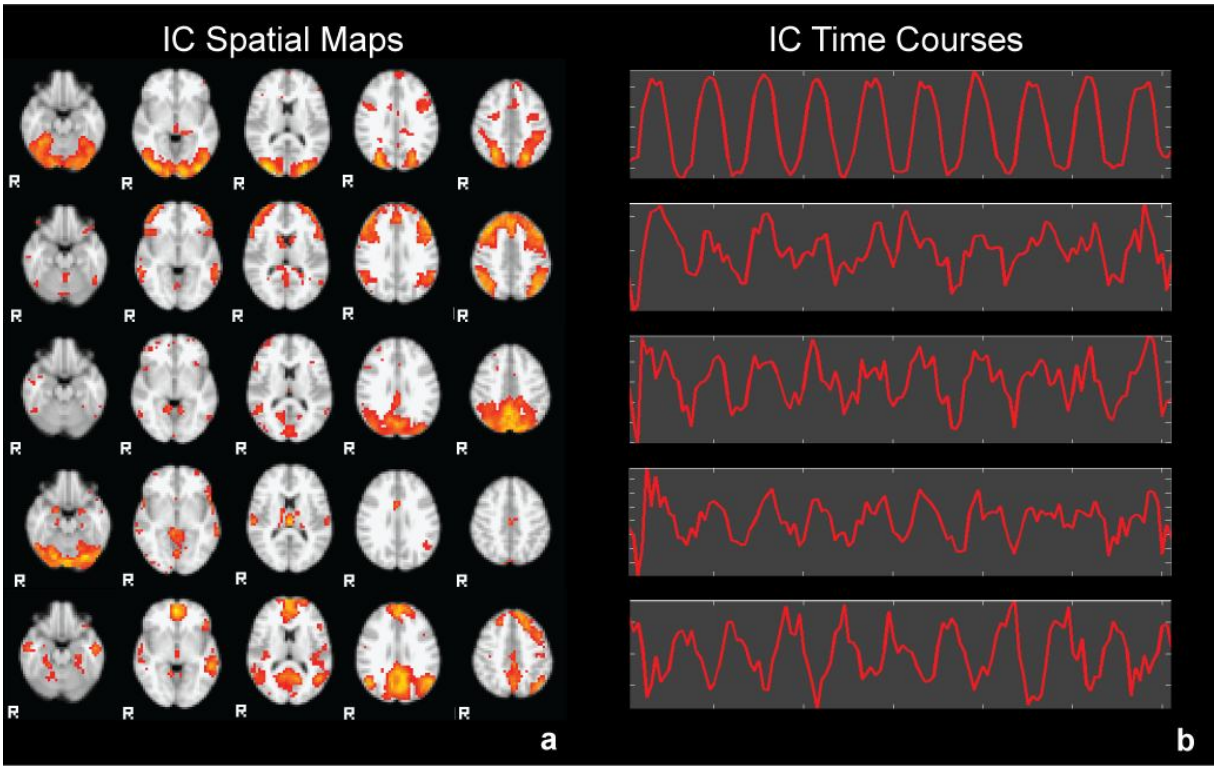

Figure 15. Estimated components in the *All_subj_age* analysis in *concat-ICA* (FWHM = 5 mm) for the Visual task. The components shown are ordered by decreasing value of correlation to the task design: (a) spatial maps (axial views at z = -20 mm, -4 mm, 12 mm, 28 mm and 44 mm) thresholded a p = 0.05 (t = 1.696, df = 31)and (b) time courses for each component.

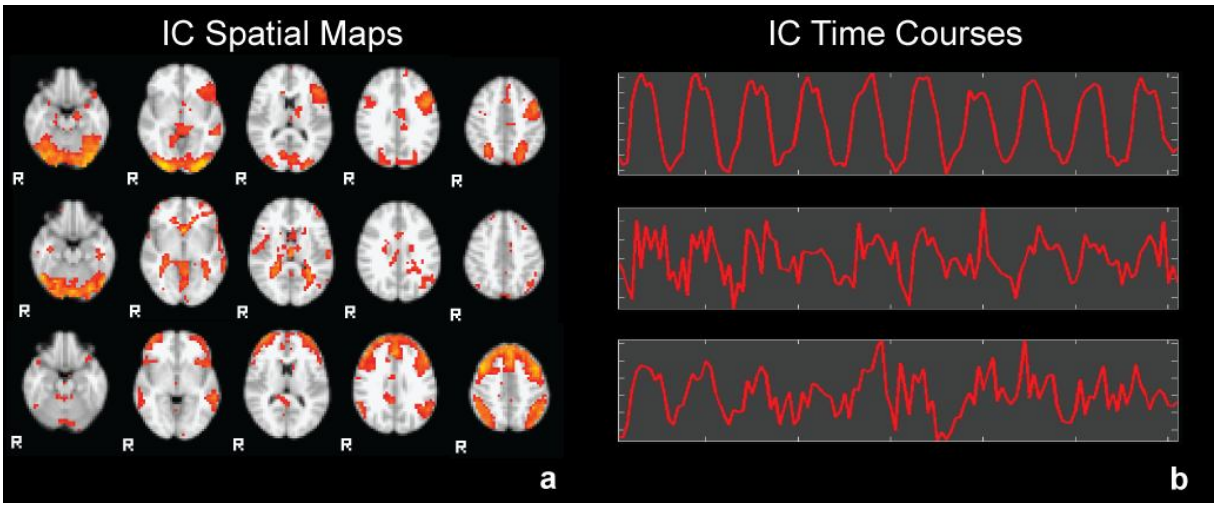

Figure 16. Estimated components in the *All_subj_age* analysis in *concat-ICA* (FWHM = 5 mm) for the Verbal task. The components shown are ordered by decreasing value of correlation to the task design: (a) spatial maps (axial views at z = -20 mm, -4 mm, 12 mm, 28 mm and 44 mm) thresholded a p = 0.05 (t = 1.697, df = 30) and (b) time courses for each component.

3.2.4. Component Sorting

The number of components of interest obtained for each analysis has been described above and a summary is presented in Table 2.

Table 2. Number of components of interest obtained for *tensor-PICA* and *concat-PICA* analyses

	Visual Encoding		Verbal Encoding	
	tensor-PICA	*concat-PICA*	*tensor-PICA*	*concat-PICA*
All_subj	4	-	2	-
All_subj_age	4	1	3	1
Matched_grps	4	3	3	1
Matched_grps_perf	4	-	3	-

When *tensor-PICA* analysis was performed using a mask to select the voxels corresponding to one of the previously estimated components of interest from *All_subj_age* analysis, significant results were obtained regarding group comparisons. The automatic estimation of the number of components yielded a total of 46, 38 and 36 components when using masks derived from components 1, 2, and 3 respectively, from Visual Encoding analysis, and 32, 16 and 35 for the masks derived from the components of interest in the Verbal Encoding analysis.

For the Visual and for the Verbal Encoding tasks, components were found that showed significant differences between the CTRL-Y and CTRL-O groups and components with significant differences between patients and controls. These results are summarised in Table 3.

Table 3. Estimated ICs that showed significant differences between groups, in analyses performed with prior masking to select the regions defined by previously estimated components.

	Visual Encoding				Verbal Encoding			
Group Comparison p<0.05	CTRL-Y>CTRL-O			CTRL-Y>RTLE CTRL-O>RTLE	CTRL-Y>CTRL-O			CTRL-Y>RTLE CTRL-O>RTLE
Mask	#1	#2	#3	#1	#1	#2	#3	#1
Automatic Dimensionality Estimation	IC1	IC6, IC7, IC8	IC8	IC9	IC4, IC7	**IC4***	IC5, IC7	IC13
20 Components	IC3	IC2, IC4	IC2, IC5, IC7	**IC7***	IC2	-	IC4	-
10 Components	-	IC2, IC4	IC3	-	-	IC2	IC2	-

* These components are shown in Figure 17.

In Figure 17 examples of two such components are shown. When using a mask derived from IC1 in the Visual task (#1 in Table 3), the seventh estimated component (analysis for 20 components) showed significant differences between controls (CTRL-Y and CTRL-O) and patients (RTLE) (Figure 17 (a) below). For the Verbal task, using a mask derived from the second component (#2 in Table 3) of *All_subj_age* analysis (Verbal task) yielded one component (the fourth) showing significant age

effects. The regions comprising this component include the hippocampus and the parahippocampal gyrus (Figure 17 (b) below).

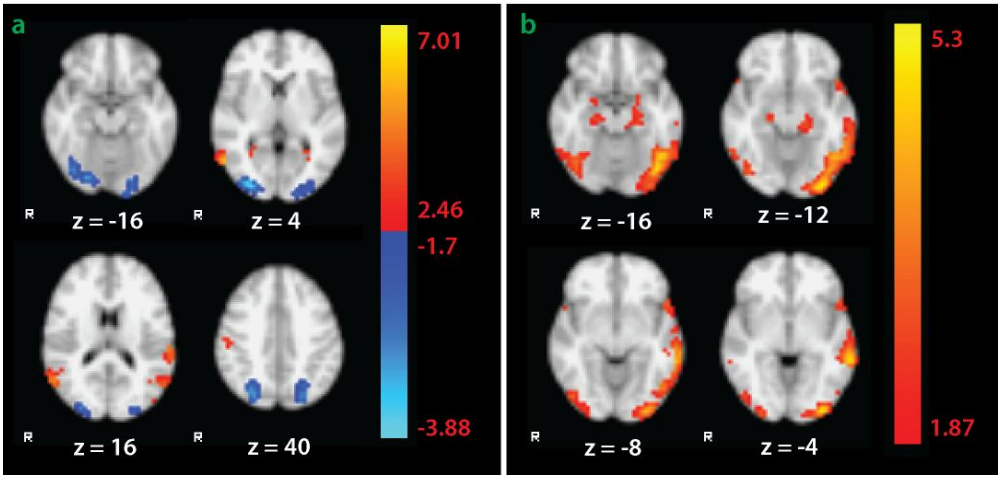

Figure 17. Networks showing significant differences between groups with *tensor-PICA* (FWHM = 5mm and alternative hypothesis threshold at p >0.5 for activation versus null): (a) component identified for the visual task using mask #1 shows significant differences between controls and patients; (b) component identified for the verbal task using mask #2 shows significant differences between older and younger controls.

For the *concat-ICA* analyses, components were ordered by performing multiple regression analysis between the IC time-courses and the task design (Figure 18), since this approach does not yield values for subject mode, like *tensor-PICA* or *concat-PICA*. Only components with r > 0.05 were considered, and those that corresponded to motion artifacts were excluded.

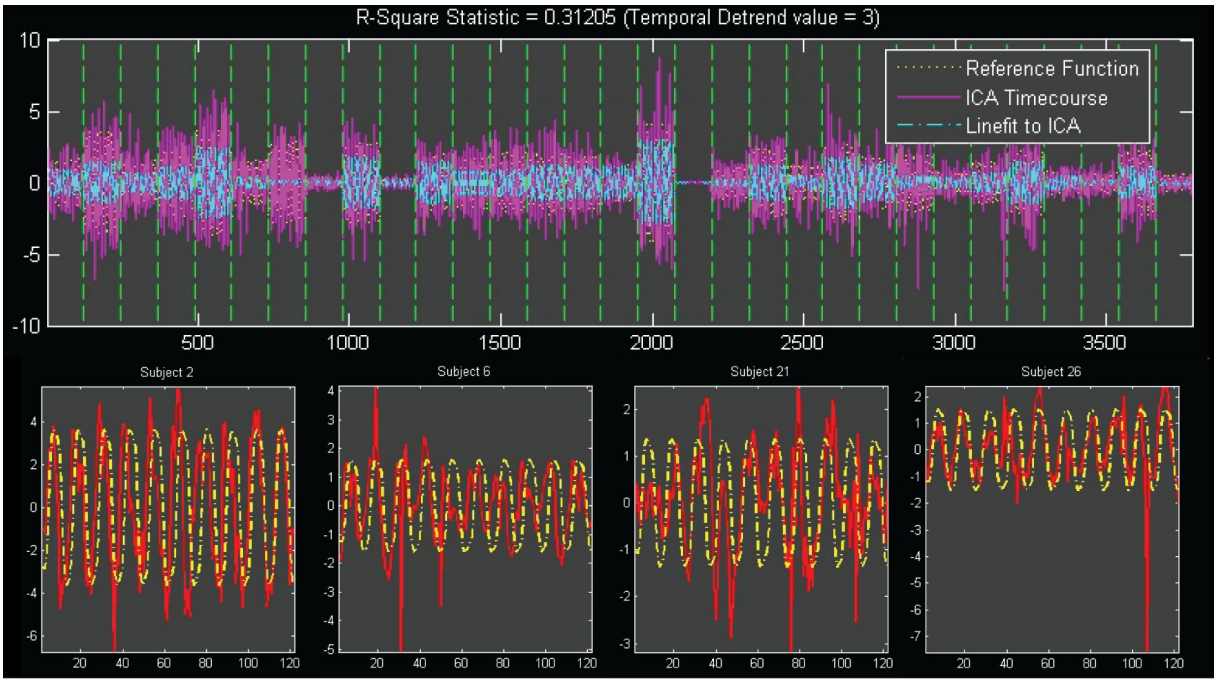

Figure 18. Example of multiple regression analysis between a component time-course (the best related component for the verbal task) and the task design: (a) concatenated time-courses for all subjects and (b)-(e) examples of individual time-courses (red line) and task design (yellow line).

4. DISCUSSION

In this section, the results obtained in the course of this work will be discussed and conclusions will be presented. Finally, possible directions of future work following this project will also be depicted.

4.1. Estimated Components

In all the analyses performed it was possible to find components comprising brain regions where activations were indeed expected, considering the task performed, namely in visual and verbal processing areas, as well as memory areas. Although the components obtained with the used methods have similarities, differences in several aspects of the output were observed. Therefore, a discussion of the components estimated with each ICA approach will be presented and comparison of the methods will be provided, in light of the obtained results.

4.1.1. Components obtained with *tensor-PICA*

In general, the analyses using *tensor-PICA* yielded interesting results in the spatial, temporal and subject domains. Components were identified that showed networks of regions whose activation was expected considering the memory tasks performed by the subjects and components unrelated to the task were isolated, such as residual motion artifacts. Regarding the pre-processing parameters, it can be concluded that, for the used datasets, performing spatial-smoothing with a Gaussian kernel of smaller FWHM (5 mm instead of 8 mm) not only yielded a higher number of components, but also allowed a better separation of source processes of interest.

4.1.2. *Concat-PICA*

When *concat-PICA* results are compared to those obtained with *tensor-PICA*, it is possible to observe that fewer components can be classified as components of interest according to the specified criterion. The datasets are the result of a block-design memory task, and consequently all subjects' time-courses are expected to be similar. In this scenario, the tensorial approach is in principle the one recommended (Beckmann and Smith 2005; Calhoun et al. 2009).

4.1.3. *Concat-ICA*

In what regards the brain regions included in the components yielded by the *concat-ICA* analyses, it was observed that these are similar to the components obtained using *concat-PICA* or *tensor-PICA*. In particular, the component that showed highest correlation with the task, as assessed by a multiple regression analysis, is comparable to the first component yielded in all other analyses. The assessment of statistical significance after the ICA decomposition within the GIFT implementation is

performed differently from the approaches using PICA. Therefore, care must be taken when comparing the results of the two approaches. However, it is possible to say that using a significance level of $p < 0.05$ to threshold the estimated spatial maps, yielded components with comparable extent of activation in most regions, in comparison with the alternative test performed within the PICA framework of $p > 0.5$ (above 50% chance of not belonging to the background noise).

4.1.4. Model-free and model-based approaches

When comparing the estimated components with the results obtained with standard GLM, it was observed that the areas showing significant activation in the GLM analyses are included in one or more of the *tensor-PICA* networks. However, the latter are generally comprised of more extensive regions, suggesting this technique may be more sensitive. Model-free analysis is of particular interest in the analysis of studies of disease or aging, since it has been discussed that the HRF in these subjects can deviate significantly from the canonical function used in most analyses. In these situations, the detection of activations using model-based techniques can be compromised by mismatch of the HRF model. In the case of *tensor-PICA*, it is also assumed that the shape of the temporal response is constant across the brain, and as a result, high variability in the temporal response can result in extra-components (Rombouts et al. 2009).

4.1.5. Resting State Networks

All of the ICA approaches used in this work yielded some components where regions inversely correlated with the tasks were identified. Among these, two patterns that correspond to resting state networks (RSNs) previously identified in the literature, namely RSN2 (for the visual task) and RSN5 (both tasks) (De Luca et al. 2006). Typically, RSN2 is described as involving the precuneus, anterior pole, structures like the hippocampus and hypothalamus and the medial parietal cortex. It has been suggested that it is involved in processes of internal monitoring and states of consciousness. The areas belonging to RSN5 are inferior regions of the parietal, occipital and prefrontal cortices, described as resembling the ventral visual pathway. (De Luca et al. 2006)

In a number of other studies using ICA, resting state networks were identified either while subjects performed a task or during rest. Since this technique is able to differentiate these patterns from those related to cardio-respiratory motion and other noise sources, it is possible that RSNs may result from some sort of neuronal activity. Nevertheless, they may be useful as a marker for functional alterations, since some studies have observed changes when comparing RSNs of normal subjects and patients (Kincses et al. 2008; Rombouts et al. 2009).

4.2. Sorting of Components

To sort out the obtained spatial maps, a set of criteria were defined to select the components of interest. Since the datasets used were obtained while subjects performed a memory task, it seems

natural that task-relatedness is one of principal criterion. In the case of a *tensor-PICA* analysis, the presented time-courses are an immediate result of the ICA decomposition, one per component for all the subjects. The comparison with the task design is then performed using a GLM approach directly on these time-courses. However, in *concat-PICA* analyses, the ICA decomposition yields a different time-course per subject, for each component. Thus, in the FSL implementation, the comparison with the task design is carried out using the best rank-1 approximation to all the time-courses of each component (Beckmann and Smith 2005). In spite of this difference, the same components are significantly task-related in both approaches ($p = 0.05$).

The other two criteria are a consequence of this being a group analysis: they try to ensure that the components of interest are relevant enough for every subject. The ICA decomposition in *tensor-PICA* yields a subject-specific value for each component that reflects the relative strength of the component. In the case of temporal concatenation, this value is estimated posterior to the analysis. Therefore it was established that only components with a relatively high median of this value across subject and non-zero value in any subject qualified as components of interest. Considering the three criteria, components were selected and it can be concluded that the tensorial approach yielded more components of interest, mainly due to their consistency across subjects.

The selected components from the *tensor-PICA* analyses were further investigated by performing masking of brain voxels prior to the ICA decomposition. This allowed the identification of smaller networks showing significant group differences. Without prior masking, the obtained components had only revealed group differences that were almost significant, which leads to the conclusion that this step increased the sensitivity of the group comparison analysis, as expected. Some of the obtained networks showed a significant age effect within normal subjects. Also, differences between normal subjects and patients were found in a network including the occipital pole and lateral occipital cortex, and deactivations in the middle temporal gyrus (RSN5).

4.3. Final remarks and future work

Overall, the work presented in this Thesis can contribute towards a protocol to guide the use of ICA in the group analysis of fMRI data. Furthermore, our results show that ICA decomposition adds valuable information about a given experiment that was not obtained with the use of standard GLM alone. Being a data-driven approach, it is of particular relevance in the analysis of data from disease studies, where there is higher inter-subject variability and haemodynamic responses can significantly differ from standard. This renders the design of an appropriate model a complex task, and may diminish the sensitivity of model-based methods. Group ICA analyses can thus be used to point out changes in brain networks in diseases, such as epilepsy or AD, which would otherwise be unnoticed or detected only at a later stage.

By comparing two different ICA algorithms (PICA vs. ICA) and two different group analyses approaches (tensorial vs. concatenation) we found that the networks of interest were consistently

obtained in every case. However, we observed that the *tensor*-PICA method was more sensitive for the detection of connectivity group differences than *concat*-PICA.

Regarding the component sorting method, we have explored the potential of using the components identified in a first ICA decomposition as masks for a second ICA. We found that the sensitivity for the detection of connectivity group differences was improved with this procedure. However, it is necessary to test the sorting criteria and the masking step in datasets from different studies, if possible with increased number of subjects, in order to be able to conclude about the improvements in the statistical significance of group differences. Additionally, the masking step was not applied to a temporal concatenation analysis, which would be of importance to better compare the two approaches.

It would also be interesting to apply the protocol to data of a resting state study, where the criteria for component selection would have to be adjusted to become independent of task-relatedness, and in which case the temporal concatenation approach is said to be more appropriate. In what regards the *concat-ICA* analyses, it is possible to conclude that the identified components are similar, but any other comparisons would be premature. It would be advisable to use the time-courses estimated to test for significant group differences that might be detected with this approach. In the future, it would also be interesting to select the components of interest by comparing them with anatomical masks of regions where activation (or deactivation) is expected or desired.

Finally, the connectivity study here presented could be further completed by performing effective connectivity analyses based on the results obtained, using methods such as Dynamic Causal Modelling (DCM) (Friston et al. 2003) or Granger Causality (Rogers et al. 2007). In particular, these could be used to evaluate the effective connectivity between the MTL and visual cortex, and also between regions in the prefrontal cortex that showed activations by measuring the relative strength as well as the direction of the connections between the activated or deactivated areas.

References

Akaike, H. (1974). "A New Look at Statistical Model Identification." *IEEE Trans Automatic Control*, 19, 716-723.

Bai, F., Zhang, Z., Watson, D. R., Yu, H., Shi, Y., Yuan, Y., Zang, Y., Zhu, C., and Qian, Y. (2009). "Abnormal Fuctional Connectivity of Hippocampus During Episodic Memory Retrieval Processing Network in Amnestic Mild Cognitive Impairment." *Biological Psychiatry*, 65, 951-958.

Beckmann, C. F., Jenkinson, M., and Smith, S. M. (2003). "General Multi-Level Linear Modelling for Group Analysis in FMRI." *NeuroImage*, 20, 1052-1063.

Beckmann, C. F., and Smith, S. M. (2004). "Probabilistic Independent Component Analysis for Functional Magnetic Resonance Imaging." *IEEE Transactions on Medical Imaging*, 23(2), 137-152.

Beckmann, C. F., and Smith, S. M. (2005). "Tensorial Extensions of Independent Component Analysis for Multisubject FMRI Analysis." *NeuroImage*, 25(1), 294-311.

Bell, A., and Sejnowski, T. J. (1995). "An Information-Maximization Approach to Blind Separation and Blind Deconvolution." *Neural Comput*, 7(6), 1129-1159.

Calhoun, V. D., Adali, T., Pearlson, G. D., and Pekar, J. J. (2001). "A Method for Making Group Inferences from Functional MRI Data Using Independent Component Analysis." *Human Brain Mapping*, 14, 140-151.

Calhoun, V. D., Liu, J., and Adali, T. (2009). "A Review of Group ICA for fMRI Data and ICA for Joint Inference of Imaging, Genetic, and ERP Data." *NeuroImage*, 45(1 Suppl), S163-S172.

Collins, D. L., Neelin, P., Peters, T. M., and Evans, A. C. (1994). "Automatic 3D Inter-Subject Registration of MR Volumetric Data in Standardized Talairach Space." *J Comput Assist Tomogr*, 18, 192-205.

De Luca, M., Beckmann, C. F., De Stefano, N., Matthews, P. M., and Smith, S. M. (2006). "fMRI Resting State Networks Define Distinct Modes of Long-Distance Interactions in the Human Brain." *NeuroImage*, 29, 1359-1367.

Desgranges, B., Baron, J., and Eustache, F. (1998). "The Functional Neuroanatomy of Episodic Memory: Ther Role of the Frontal Lobes, the Hippocampal Formation, and Other Areas." *NeuroImage*, 8, 198-213.

Dudai, Y. (2002). *Memory from A to Z - Keywords, Concepts and Beyond*, Oxford University Press.

Figueiredo, P., Santana, I., Teixeira, J., Cunha, C., Machado, E., Sales, F., Almeida, E., and Castelo-Branco, M. (2008). "Adaptive Visual Memory Reorganization in Right Medial Temporal Lobe Epilepsy." *Epilepsia*, 49(8), 1395-1408.

Friston, K. J., Harrison, L., and Penny, W. (2003). "Dynamic Causal Modelling." *NeuroImage*, 19, 1273-1302.

Huettel, S. A., Song, A. W., and McCarthy, G. (2004). *Functional Magnetic Resonance Imaging*, Sinauer Associates, Inc.

Hyvärinen, A. (1999). "Fast and robust fixed-point algorithms for independent component analysis." *IEEE Transactions on Neural Networks*, 10(3), 626-634.

Hyvärinen, A., and Oja, E. (2000). "Independent Component Analysis: Algorithms and Applications." *Neural Networks*, 13(4-5), 411-430.

Jenkinson, M., Bannister, P., Brady, M., and Smith, S. M. (2002). "Improved Optimisation for the Robust and Accurate Linear Registration and Motion Correction of Brain Images." *NeuroImage*, 17(2), 825-841.

Jenkinson, M., and Smith, S. M. (2001). "A Global Optimisation Method for Robust Affine Registration of Brain Images." *Medical Image Analysis*, 5(2), 143-156.

Jezzard, P., and Clare, S. (2001). "Principles of Nuclear Magnetic Resonance and MRI. Ch 3." Functional MRI: An Introduction to Methods, P. Jezzard, P. M. Matthews, and S. M. Smith, eds., Oxford University Press, 67-92.

Kandell, E. R., Schwartz, J. H., and Jessel, T. M. (2000). *Principles of Neural Science*, McGraw-Hill.

Kincses, Z. T., Johansen-Berg, H., Tomassini, V., Bosnell, R., Matthews, P. M., and Beckmann, C. F. (2008). "Model-Free Characterization of Brain Functional Networks for Motor Sequence Learning Using fMRI." *NeuroImage*, 39, 1950-1958.

Lavenex, P., and Amaral, D. G. (2000). "Hippocampal-Neocortical Interaction: A Hierarchy of Associativity." *Hippocampus*, 10(420-430).

Li, K., Guo, L., Nie, J., Li, G., and Liu, T. (2008). "Review of Methods for Functional Connectivity Detection Using fMRI." *Computerized Medical Imaging and Graphics*, 33, 131-139.

Logothetis, N. K., and Wandell, B. A. (2004). "Interpreting the BOLD Signal." *Annual Review Physiology*, 66, 735-769.

Matthews, P. M. (2001). "An Introduction to Functional Magnetic Resonance Imaging of the Brain. Ch 1." Functional MRI: An Introduction to Methods, P. Jezzard, P. M. Matthews, and S. M. Smith, eds., Oxford University Press.

Mazziotta, J., Toga, A., Evans, A., Fox, P., Lancaster, J., Zilles, K., Woods, R., Paus, T., Simpson, G., Pike, B., Holmes, C., Collins, L., Thompson, P., MacDonald, D., Iacoboni, M., Schormann, T., Amunts, K., Palomero-Gallagher, N., Geyer, S., Parsons, L., Narr, K., Kabani, N., Le Goualher, G., Boomsma, D., Cannon, T., Kawashima, R., and Mazoyer, B. (2001). "A Probabilistic Atlas and Reference System for the Human Brain: International Consortium for Brain Mapping (ICBM)." *Philos Trans R Soc Lond B Biol Sci*, 356(1412), 1293–1322.

McKeown, M. J., Makeig, S., Brown, G., Jung, T., Kindermann, S. S., Bell, A., and Sejnowski, T. J. (1998). "Analysis of fMRI Data by Blind Separation Into Independent Spatial Components." *Human Brain Mapping*, 6, 160–188.

Menon, R. S., Ogawa, S., Hu, X., Strupp, J. P., Anderson, P., and Ugurbil, K. (1995). "BOLD Based Functional MRI at 4 Tesla Includes a Capillary Bed Contribution: Echo-Planar Imaging Correlates with Previous Optical Imaging Using Intrinsic Signals." *Magn. Reson. Med.*, 33(3), 453-459.

Minka, T. (2000). "Automatic Choice of Dimensionality for PCA. Technical Report 514." MIT Media Lab Vision and Modeling Group.

Ogawa, S., and Lee, T. M. (1990). "Magnetic Resonance Imaging of Blood Vessels at High Fields: In Vivo and In Vitro Measurements and Image Simulation." *Magn. Reson. Med.*, 16(1), 9-18.

Ogawa, S., Lee, T. M., Nayak, A. S., and Glynn, P. (1990). "Oxygenation-Sensitive Contrast in Magnetic Resonance Image of Rodent Brain at High Magnetic Fields." *Magn. Reson. Med.*, 14(1), 68-78.

Ramnani, N., Behrens, T. E. J., Penny, W., and Matthews, P. M. (2004). "New Approaches for Exploring Anatomical and Functional Connectivity in the Human Brain." *Biological Psychiatry*, 56, 613-619.

Ramnani, N., Lee, L., Mechelli, A., Phillips, C., Roebroeck, A., and Formisano, E. (2002). "Exploring Brain Connectivity: a New Frontier in Systems Neurosciences." *Trends in Neurosciences*, 25(10).

Ranganath, C., Heller, A., Cohen, M. X., Brozinsky, C. J., and Rissman, J. (2005). "Functional Connectivity with the Hippocampus During Successful Memory Formation." *Hippocampus*, 15, 997-1005.

Rissanen, J. (1983). "A Universal Prior for Integers and Estimation by Minimum Description Length." *Ann Statistics*, 11, 416-431.

Rogers, B. P., Morgan, V. L., Newton, A. T., and Gore, J. C. (2007). "Asssessing Functional Connectivity in the Human Brain by fMRI." *Magnetic Resonance Imaging*, 25(10), 1347-1357.

Rombouts, S. A., Damoiseaux, J. S., Goekoop, R., Barkhof, F. S., P, Smith, S. M., and Beckmann, C. F. (2009). "Model-Free Group Analysis Shows Altered BOLD FMRI Networks in Dementia." *Human Brain Mapping*, 30, 256-266.

Smith, S. M. (2002). "Fast Robust Automated Brain Extraction." *Human Brain Mapping*, 17(3), 143-155.

Squire, L. R. (2004). "Memory Systems of the Brain: A Brief History and Current Perspective." *Neurobiology of Learning and Memory*, 82, 171-177.

Summerfield, C., Greene, M., Wager, T., Egner, T., Hirsch, J., and Mangels, J. (2006). "Neocortical Connectvity During Episodic Memory Formation." *PLoS Biology*, 4(5), e128.

Tipping, M. E., and Bishop, C. M. (1999). "Probabilistic Principal Component Analysis." *J Royal Statistical Society B*, 61(3).

Voets, N. L., Adcock, J. E., Stacey, R., Hart, Y., Carpenter, K., Matthews, P. M., and Beckmann, C. F. (2009). "Functional and Structural Changes in the Memory Network Associated With Left Temporal Lobe Epilepsy." *Human Brain Mapping*.

Wang, L., Zang, Y., He, Y., Liang, M., Zhang, X., Tian, L., Wu, T., Jiang, T., and Li, K. (2006). "Changes in Hippocampal Connectivity in the Early Stages of Alzheimer's Disease: Evidence from Resting State fMRI." *NeuroImage*, 31, 496-504.

Woolrich, M. W., Behrens, T. E. J., Beckmann, C. F., Jenkinson, M., and Smith, S. M. (2004). "Multi-Level Linear Modelling for FMRI Group Analysis Using Bayesian Inference." *NeuroImage*, 21(4), 1732-1747.

Woolrich, M. W., Ripley, B. D., Brady, M., and Smith, S. M. (2001). "Temporal Autocorrelation in Univariate Linear Modelling of FMRI Data." *NeuroImage*, 14(6), 1370-1386.

Worsley, K. J. (2001). "Statistical analysis of activation images. Ch 14." Funtional MRI: An Introduction to Methods, P. Jezzard, P. M. Matthews, and S. M. Smith, eds., Oxford University Press.

Worsley, K. J., and Friston, K. J. (1995). "Analysis of fMRI Time-Series Revisited - Again." *NeuroImage*, 2, 173-181.

Appendix

Linux script to apply a mask before the ICA decomposition

```
#!/bin/sh

####################################
path='/home/catarina/Data/ICAData';
orig_analysis_dir='VisEnc_5_age'
component='3';

tdes='/home/catarina/Data/FeatFirstLevelRTLEs/MFA_VisualEncoding5.feat/desi
      gn.mat';
tcon='/home/catarina/Data/FeatFirstLevelRTLEs/MFA_VisualEncoding5.feat/desi
      gn.con';
sdes='/home/catarina/Data/FeatScndLevel/VisEnc5_age.gfeat/design.mat';
scon='/home/catarina/Data/FeatScndLevel/VisEnc5_age.gfeat/design.con';

mkdir ${path}/mask${component}_${orig_analysis_dir};
cd ${path}/mask${component}_${orig_analysis_dir};

odir=`pwd`;
echo $odir
####################################


##### copy necessary files

cp ${path}/${orig_analysis_dir}.gica/groupmelodic.ica/stats/
      thresh_zstat${component}.nii.gz $odir
cp ${path}/${orig_analysis_dir}.gica/bg_image.nii.gz $odir
cp ${path}/${orig_analysis_dir}.gica/.filelist $odir


##### create mask

fslmaths thresh_zstat${component}.nii.gz -abs mask_abs.nii.gz
fslmaths mask_abs.nii.gz -bin mask_bin.nii.gz


## run melodic ##
# all components
/usr/local/fsl/bin/melodic -i .filelist -o groupmelodic0.ica -v
-m mask_bin.nii.gz --nobet --bgthreshold=3 --tr=3.0 --report
--guireport=../../report.html --bgimage=bg_image -d 0 --mmthresh=0.5
--Oall -a tica --Tdes=$tdes --Tcon=$tcon --Sdes=$sdes --Scon=$scon

# 20 components
/usr/local/fsl/bin/melodic -i .filelist -o groupmelodic20.ica -v
-m mask_bin.nii.gz --nobet --bgthreshold=3 --tr=3.0 --report
--guireport=../../report.html --bgimage=bg_image -d 20 --mmthresh=0.5
--Oall -a tica --Tdes=$tdes --Tcon=$tcon --Sdes=$sdes --Scon=$scon

# 10 components
/usr/local/fsl/bin/melodic -i .filelist -o groupmelodic10.ica -v
-m mask_bin.nii.gz --nobet --bgthreshold=3 --tr=3.0 --report
--guireport=../../report.html --bgimage=bg_image -d 10 --mmthresh=0.5
--Oall -a tica --Tdes=$tdes --Tcon=$tcon --Sdes=$sdes --Scon=$scon
```